expression. To investigate the contribution of anti-NF-κB mediated pathways in the anti-AD effects of LR extracts, IκBα, COX-2 and iNOS were measured in the mouse epidermis by Western blot. As can be seen in Fig. 2A, IκBα was significantly decreased in the epidermis by Ox treatment, whereas COX-2 and iNOS were increased. The treatment of LR extracts (500 mg/kg) attenuated the IκBα degradation by 31% (Fig. 2B), while COX-2 and iNOS expression were inhibited by 82% (Fig. 2C) and 74% (Fig. 2D), respectively. In case of PDS, 3 mg/kg attenuated IκBα degradation by 20% and suppressed COX-2 and iNOS by 80% and 22%, respectively.

In conclusion, we demonstrated that oral administration of LR extracts can manifest anti-AD effects in chronic Ox-induced AD in mouse as shown by recovery of skin barrier disruption, serum IgE decrease and prominent clinical and histopathological improvement. Attenuation of IκB degradation and suppression of COX-2 and iNOS were shown to mediate these anti-AD effects of LR extracts. In addition, we could demonstrate that Ox-induced murine AD model can be a useful model for the evaluation of anti-AD effects of potential drug candidates for the treatment of AD.

References

[1] Leung DY, Boguniewicz M, Howell MD, Nomura I, Hamid QA. New insights into atopic dermatitis. J Clin Invest 2004;113(5):651–7.
[2] Abramovits W, Perlmutter A. Steroids versus other immune modulators in the management of allergic dermatoses. Curr Opin Allergy Clin Immunol 2006; 6(5):345–54.
[3] Staniforth V, Wang SY, Shyur LF, Yang NS. Shikonins, phytocompounds from *Lithospermum erythrorhizon*, inhibit the transcriptional activation of human tumor necrosis factor α promoter *in vivo*. J Biol Chem 2004;279(7):5877–85.
[4] Thuong PT, Kang KW, Kim JK, Seo DB, Lee SJ, Kim SH, et al. Lithospermic acid derivatives from *Lithospermum erythrorhizon* increased expression of serine palmitoyltransferase in human HaCaT cells. Bioorg Med Chem Lett 2009;19(6):1815–7.
[5] Kim EK, Kim EY, Moon PD, Um JY, Kim HM, Lee HS, et al. Lithospermi radix extract inhibits histamine release and production of inflammatory cytokine in mast cells. Biosci Biotechnol Biochem 2007;71:2886–92.
[6] Kim J, Kim H, Jeong do H, Kim SH, Park SK, Cho Y. Comparative effect of gromwell (*Lithospermum erythrorhizon*) extract and borage oil on reversing epidermal hyperproliferation in guinea pigs. Biosci Biotechnol Biochem 2006;70(9):2086–95.
[7] Man MQ, Hatano Y, Lee SH, Man M, Chang S, Feingold KR, et al. Characterization of a hapten-induced, murine model with multiple features of atopic dermatitis: structural, immunologic, and biochemical changes following single versus multiple oxazolone challenges. J Invest Dermatol 2008;128:79–86.
[8] Han KY, Kwon TH, Lee TH, Lee SJ, Kim SH, Kim J. Suppressive effects of *Lithospermum erythrorhizon* extracts on lipopolysaccharide-induced activation of AP-1 and NF-kappaB via mitogen-activated protein kinase pathways in mouse macrophage cells. BMB Rep 2008;41(4):328–33.
[9] Lee KM, Kang BS, Lee HL, Son SJ, Hwang SH, Kim DS, et al. Spinal NF-κB activation induces COX-2 upregulation and contributes to inflammatory pain hypersensitivity. Eur J Neurosci 2004;19(12):3375–81.
[10] Lim KM, Lee JY, Lee SM, Bae ON, Noh JY, Kim EJ, et al. Potent anti-inflammatory effects of two quinolinedione compounds, OQ1 and OQ21, mediated by dual inhibition of inducible NO synthase and cyclooxygenase-2. Br J Pharmacol 2009;156(2):328–37.

Ji Hae Lee, Kyoung-Mi Jung, Il-Hong Bae, SiYoung Cho, Dae-Bang Seo, Sang-Jun Lee, Young-Ho Park, Kyung-Min Lim*
Amorepacific Corporation R&D Center, 314-1 Boradong, Giheung-gu, Yongin-si, Gyeonggi-do 449-729, Republic of Korea

*Corresponding author. Tel.: +82 31 280 5904; fax: +82 31 281 8390
E-mail address: kimlim@amorepacific.com (Kyung-Min Lim)

19 March 2009

doi:10.1016/j.jdermsci.2009.07.001

Letter to the Editor

The compound heterozygote for new/recurrent *COL7A1* mutations in a Japanese patient with bullous dermolysis of the newborn

To the Editor,

Transient bullous dermolysis of the newborn (TBDN; OMIM 131705) is a rare genodermatosis characterized by mucocutaneous blisters and erosions at birth, which remit spontaneously within several months with minimal scarring. About 30 cases of this disorder have been reported thus far. According to the publication in 2008 for the Third International Consensus Meeting on Diagnosis and Classification of Epidermolysis Bullosa, it was recommended that the name TBDN be changed to "bullous dermolysis of the newborn (BDN)" because the disease is not always transient, and rare patients continue to blister beyond the newborn period [1]. Immunofluorescence with anti-type VII collagen antibody reveals a granular pattern within the epidermis. Ultrastructural examination reveals separation of the dermal–epidermal junction below the lamina densa, impaired anchoring fibrils in reduced numbers, and dilated rough endoplasmic reticulum containing electron-dense stellate bodies in basal and some suprabasal keratinocytes. Thus, BDN is thought to be a rare form of dystrophic epidermolysis bullosa (DEB). DEB results from mutations in *COL7A1*, encoding type VII collagen, which is the major component of anchoring fibrils at the dermal–epidermal junction. Over 300 different mutations have been reported throughout the world. Recent genetic investigations in four families have shown that BDN also results from *COL7A1* mutations [2–5]. In this study, we investigated *COL7A1* gene pathology in an additional Japanese patient with BDN and identified compound heterozygous new/recurrent mutations.

The patient was a male infant who was the offspring of healthy unrelated Japanese parents. At birth, widespread blisters and erosions were noted on the trunk and extremities (Fig. 1A). Three months later, the tendency to form blisters decreased and erosions healed with milia (Fig. 1B). Light microscopy revealed subepidermal blisters. Immunofluorescence with anti-type VII collagen monoclonal antibody showed granular deposits within basal keratinocytes and slight reduction of linear staining at the dermal–epidermal junction (Fig. 1C). Electron microscopy revealed blister formation beneath the lamina densa. Examination of unblistered dermal–epidermal junctions showed poorly formed anchoring fibrils present at reduced numbers and containing large granular perinuclear inclusions (stellate bodies) in basal keratinocytes (Fig. 1D). These features suggested a diagnosis of BDN. By one year of age, no further blister formation occurred. However, minimal scarring and nail dystrophy remained present.

All described studies were performed following permission from the medical ethical committee of Kurume University School of Medicine. Written informed consent was obtained from the patient's legal guardian and the study was conducted according to the Declaration of Helsinki Principles. Genomic DNA from the patient was extracted from peripheral blood using standard methods. For mutation analysis, polymerase chain reaction (PCR) fragments were amplified with pairs of primers spanning all 118 exons of *COL7A1*. The mutation detection strategy consisted of heteroduplex scanning by conformation-sensitive gel electro-

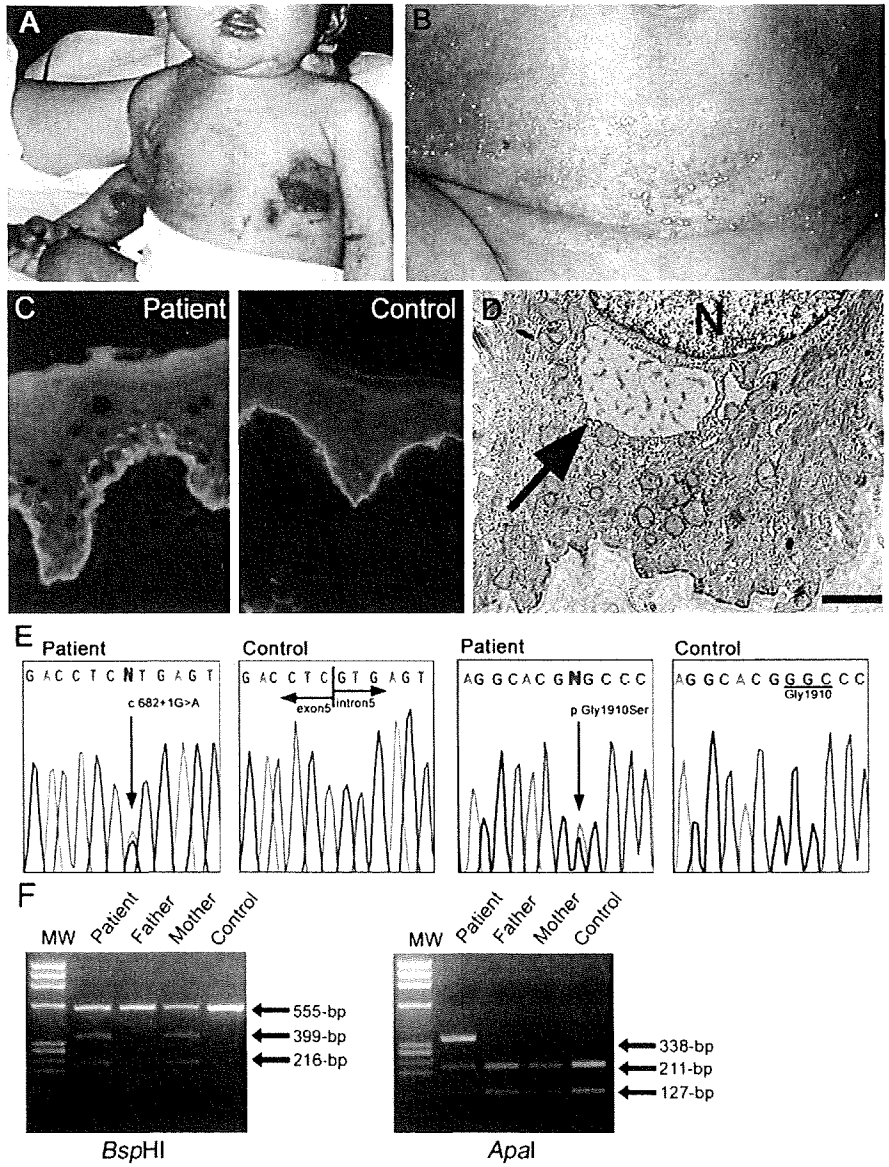

Fig. 1. BDN patient in the present study. (A) Widespread blistering and erosions on the trunk and extremities at birth. (B) Blisters and erosions healed, with many milia at the age of three months; no further blister formation visible. (C) Anti-type VII collagen monoclonal antibody LH 7:2 immunofluorescent staining of skin from the patient showing a widespread punctate and granular pattern within the epidermis and markedly reduced linear staining at the dermal–epidermal junction, compared to the normal control skin (original magnification 200×). (D) Transmission electron microscopy showing a large granular perinuclear inclusion (stellate body) within the basal keratinocyte cytoplasm (arrow), as well as reduced numbers of poorly formed anchoring fibrils. N, nucleus; bar = 1 μm. (E) Direct sequencing of the patient's *COL7A1* gene showing compound heterozygosity for a donor splice site/missense combination mutation: c.682+1G>A and p.Gly1910Ser. (F) Restriction endonuclease digestion of PCR products using BspHI (left) and ApaI (right). The left panel shows that the heterozygous DNA containing the mutation c.682+1G>A (patient and mother) digested into fragments of 399- and 216-bp in size. By contrast, there is an additional undigested band of 555-bp in amplified mutant DNA. The PCR products from the father and control show the absence of a solitary BspHI cut-site. The right panel shows that the heterozygous DNA containing the mutation p.Gly1910Ser (patient only) has the absence of a solitary ApaI cut-site. There are additional digested bands of 211- and 127-bp in amplified mutant DNA. The PCR products from the father, mother and control digested into fragments of 211- and 127-bp in size.

phoresis. The corresponding PCR products showing heteroduplexes were sequenced using Big Dye labeling in an ABI310 genetic analyzer (Applied Biosystems, Foster City, CA). Direct nucleotide sequencing identified compound heterozygosity for a donor splice site/missense combination of mutations; i.e., c.682+1G>A and p.Gly1910Ser (GenBank NM_000094) (Fig. 1E). The c.682+1G>A was found in genomic DNA from the mother. Whereas the p.Gly1910Ser variant was not found in genomic DNA from the father, suggesting that it represented *de novo* mutations. These mutations were confirmed by restriction endonuclease digestion (Fig. 1F). The p.Gly1910Ser mutation has not been reported previously and this variant was not detected in 100 ethnically matched controls. Neither mutation has been described before in BDN, although the c.682+1G>A mutation had been identified in a patient with severe generalized recessive DEB [6].

The etiology of BDN is currently unknown. Immunofluorescence with anti-type VII collagen antibody demonstrates a strikingly weak staining on the basement membrane, but a strong

Table 1
COL7A1 mutations published to date in patients with BDN (including this case).

Mutation	Inheritance	Location	Protein domain	Consequences	Reference
c.4120-1G>C	AD	Intron 35	THC	In-frame exon skipping	[2]
p.Gly1519Asp/p.Gly2551Glu	AR	Exon 44/Exon 86	THC/THC	GS/GS	[3]
p.Gly1522Glu	AD	Exon 45	THC	GS	[4]
c.5504delA/p.Arg2008His	AR	Exon 64/Exon 73	THC/THC	PTC/missense	[5]
c.682+1G>A/p.Gly1910Ser	AR	Intron 5/Exon 68	CMP/THC	PTC/GS	This case

Abbreviations: AD, autosomal dominant; AR, autosomal recessive; THC, triple helical collagenous domain; CMP, cartilage matrix protein; GS, glycine substitution; PTC, premature termination codon.

intracellular staining in basal and suprabasal keratinocytes, although similar findings have been reported in other forms of DEB. Interestingly, these abnormal findings revert to linear distribution along the dermal–epidermal junction, with focal intraepidermal deposits of type VII collagen within some basal keratinocytes, following cessation or at least marked reduction in the intensity and frequency of blistering [4]. On ultrastructural examination, the stellate bodies within dilated rough endoplasmic reticulum also correspond to intraepidermal deposits of type VII collagen.

So far, six different *COL7A1* mutations have been described in four families with BDN with either an autosomal dominant or an autosomal recessive inheritance, as detailed in Table 1. The p.Gly1522Glu and c.5504delA in six mutations have been reported previously in patients with other forms of DEB, DEB pruriginosa and generalized other recessive DEB, respectively [7,8].

Here, we studied a Japanese patient with BDN who manifested compound heterozygous mutations c.682+1G>A and p.Gly1910-Ser in *COL7A1*. Dominant DEB has been shown predominantly to be associated with glycine substitutions (GS) within the triple helical collagenous domain of type VII collagen. The heterozygous GS interfere with the triple helical assembly of type VII collagen, leading to milder dominant phenotypes. However, some GS are 'silent' in the heterozygous state and cause disease only when combined with another *COL7A1* mutation [9]. The p.Gly1519Asp mutation has been reported previously as a 'silent' GS in a patient with BDN [3]. Because p.Gly1910Ser was not found in genomic DNA from the unaffected father, it is not clear whether p.Gly1910Ser is a pathogenic or 'silent' GS in the present case. The other mutation c.682+1G>A in this study has previously been described in a patient with severe generalized recessive DEB [6]. Analysis of this mutation in the patient's mRNA revealed a mutant transcript with inclusion of the entire intron 5 as a new exon, leading to a premature termination codon (PTC) and nonsense-mediated mRNA decay. The clinical consequences of recessively inherited pathogenic or 'silent' GS combined with PTC are mild, moderate or severe recessive DEB [9]. Although our patient is the first case of compound heterozygosity for a GS/PTC combination of *COL7A1* mutations in BDN, there does not appear to be any clear paradigm for genotype–phenotype correlation.

Pathological features of BDN and molecular mechanisms remain unclear. Further investigations will be necessary to define the skin pathology of this genodermatosis.

Acknowledgments

We thank the patient for his participation. This work was supported by a Grant-in-Aid for Scientific Research from the Ministry of Education, Culture, Sports, Science and Technology of Japan, by Health Science Grants for Research on Scientific Disease from the Ministry of Health, Labor and Welfare of Japan, by an Open Research Center Project of the Ministry of Education, Culture, Sports, Science and Technology of Japan, and by a Kaibara Morikazu Medical Science Promotion Foundation.

References

[1] Fine JD, Eady RA, Bauer EA, Bauer JW, Bruckner-Tuderman L, Heagerty A, et al. The classification of inherited epidermolysis bullosa (EB): report of the Third International Consensus Meeting on Diagnosis and Classification of EB. J Am Acad Dermatol 2008;58:931–50.
[2] Christiano AM, Fine JD, Uitto J. Genetic basis of dominantly inherited transient bullous dermolysis of the newborn: a splice site mutation in the type VII collagen gene. J Invest Dermatol 1997;109:811–4.
[3] Hammami-Hauasli N, Raghunath M, Küster W, Bruckner-Tuderman L. Transient bullous dermolysis of the newborn associated with compound heterozygosity for recessive and dominant COL7A1 mutations. J Invest Dermatol 1998;111:1214–9.
[4] Fassihi H, Diba VC, Wessagowit V, Dopping-Hepenstal PJ, Jones CA, Burrows NP, et al. Transient bullous dermolysis of the newborn in three generations. Br J Dermatol 2005;153:1058–63.
[5] Nakano H, Toyomaki Y, Ohashi S, Nakano A, Jin H, Munakata T, et al. Novel *COL7A1* mutations in a Japanese family with transient bullous dermolysis of the newborn associated with pseudosyndactyly. Br J Dermatol 2007;157:179–82.
[6] Hovnanian A, Rochat A, Bodemer C, Petit E, Rivers CA, Prost C, et al. Characterization of 18 new mutations in COL7A1 in recessive dystrophic epidermolysis bullosa provides evidence for distinct molecular mechanisms underlying defective anchoring fibril formation. Am J Hum Genet 1997;61:599–610.
[7] Whittock NV, Ashton GH, Mohammedi R, Mellerio JE, Mathew CG, Abbs SJ, et al. Comparative mutation detection screening of the type VII collagen gene (COL7A1) using the protein truncation test, fluorescent chemical cleavage of mismatch, and conformation sensitive gel electrophoresis. J Invest Dermatol 1999;113:673–86.
[8] Ishiko A, Masunaga T, Ota T, Nishikawa T. Does the position of the premature termination codon in COL7A1 correlate with the clinical severity in recessive dystrophic epidermolysis bullosa? Exp Dermatol 2004;13:229–33.
[9] Uitto J, Pulkkinen L, Christiano A. The molecular basis of the dystrophic forms of epidermolysis bullosa. In: Fine JD, Bauer EA, McGuire J, Moshell A, editors. In Epidermolysis Bullosa. Baltimore: The Johns Hopkins University Press; 1999. p. 326–50.

Keiko Hashikawa[a], Takahiro Hamada[a,*], Norito Ishii[a], Shunpei Fukuda[a], Rie Kuroki[b], Takekuni Nakama[a], Shinichiro Yasumoto[a], Katsuto Tamai[c], Hajime Nakano[d], Daisuke Sawamura[d], Takashi Hashimoto[a]
[a]*Department of Dermatology, Kurume University School of Medicine, 67 Asahimachi, Kurume 830-0011, Japan*
[b]*Division of Dermatology, Fukuoka Tokusyukai Medical Center, Kasuga, Japan*
[c]*Division of Gene Therapy Science, Department of Molecular Therapeutics, Osaka University Graduate School of Medicine, Osaka, Japan*
[d]*Department of Dermatology, Hirosaki University Graduate School of Medicine, Hirosaki, Japan*

*Corresponding author. Tel.: +81 942 31 7571; fax: +81 942 34 2620
E-mail address: hamataka@med.kurume-u.ac.jp (Takahiro Hamada)

13 April 2009

doi:10.1016/j.jdermsci.2009.06.011

TISSUE ENGINEERING: Part A
Volume 00, Number 00, 2010

DOI: 10.1089/ten.tea.2009.0322

Original Article

Controlled Release of Bone Morphogenetic Protein-2 Enhances Recruitment of Osteogenic Progenitor Cells for *De Novo* Generation of Bone Tissue

Yu Kimura, Ph.D.,[1] Nobuhiko Miyazaki, M.Eng.,[1] Naoki Hayashi, M.Eng.,[1]
Satoru Otsuru, M.D., Ph.D.,[2] Katsuto Tamai, M.D., Ph.D.,[2] Yasufumi Kaneda, M.D., Ph.D.,[2]
and Yasuhiko Tabata, Ph.D., D.Med.Sci., D.Pharm.[1]

The objective of this study was to evaluate the cellular contribution to the phenomenon of *de novo* generation of bone tissue induced by the controlled release of bone morphogenetic protein-2 (BMP-2). Gelatin hydrogels (2 mg) incorporating BMP-2 (3 μg) with different water contents were subcutaneously implanted into the back of enhanced green fluorescent protein-chimeric mice to induce the ectopic *de novo* generation of bone tissue. The hydrogels incorporating BMP-2 could release BMP-2 at different time profiles. When evaluated radiologically and histologically, the ectopic *de novo* generation of bone tissue was induced by the controlled release of BMP-2 from the hydrogels around the hydrogel-implanted site. The relative percentage number of green fluorescent protein- to osteocalcin-positive cells recruited into the *de novo* generated bone tissue depended on the BMP-2 release profile. The higher the percentage, the stronger was the *de novo* generation of bone tissue. These findings indicate that bone marrow-derived osteoblast progenitor cells were recruited from the blood circulation by BMP-2 release and consequently contributed to the ectopic *de novo* generation of bone tissue. It is conceivable that the local concentration of BMP-2 modifies the recruitment profile of progenitor cells with an osteogenic potential around the release site of BMP-2, resulting in regulated volume of *de novo* generated bone tissue.

Introduction

TISSUE ENGINEERING has been vigorously investigated over the last 20 years to experimentally demonstrate the biomedical feasibility of regeneration in medical therapy. The key components are cells, the scaffolds for cells attachment, proliferation, or differentiation, and biosignaling molecules for cell proliferation and differentiation. Various precursor or stem cells have been extensively studied and the mechanisms of their differentiation into specific cell lineages have been clarified recently.[1,2] Among the well-recognized mechanisms, it has been demonstrated that several soluble factors interact with their cellular receptor and subsequently start the intracellular signals required for specific gene expression. In addition, the matrix present around cells, so-called extracellular matrix, also plays an important role in the activation of signals and their biological functions.[3–5]

Recently, some research reports strongly suggest that stem or precursor cells circulating in the blood and body are originally present for hematopoiesis, vascularization, or mesenchymal tissue regeneration.[6–15] Therefore, it is highly conceivable that a promoted recruitment of cells that are inherently present in the body to a body site results in cell-based tissue regeneration at the site. If the *in vivo* recruitment or fate of cells can be regulated by making use of their recruitment mechanism, tissue regeneration based on the cells present in the body can be achieved. We have developed gelatin hydrogels for the controlled release of various biosignaling molecules, such as growth factors, chemokines, and genes, and succeeded in the regeneration and repairing of various tissues.[16] Among them, it is well-known that bone morphogenetic protein-2 (BMP-2) is a strong inducer of bone tissue formation through mesenchymal cell infiltration, differentiation of mesenchymal cells into chondrocytes, diminishment of chondroid tissue, and generation of bone tissue.[17–19] Many researches have been reported for the complete regeneration of bone tissue with BMP-2.[20] In addition, it has been reported that BMP-2 is able to enhance the cells' mobilization.[21] This activity is promising and useful from the viewpoint that tissue regeneration can be achieved through the recruitment of cells originally present in the body.

[1]Department of Biomaterials, Institute for Frontier Medical Sciences, Kyoto University, Kyoto, Japan.
[2]Department of Molecular therapeutics, Graduate School of Medicine, Osaka University, Osaka, Japan.

The objective of this study was to evaluate BMP-2-induced *de novo* generation of bone tissue in terms of cell recruitment. Previous research reports have demonstrated the contribution of bone marrow for bone fracture healing through hematoma formation.[22–25] Although they indicated the possible contribution of growth factors in hematoma or bone marrow cells to fracture healing, the characterization of cells contributing for *de novo* generation of bone tissue was not clarified. In this study, BMP-2 was incorporated into gelatin hydrogels with different degradabilities for the controlled release in different profiles. After the hydrogels incorporating BMP-2 were implanted subcutaneously, ectopic *de novo* generation of bone tissue was evaluated by radiological and histological examinations. We examined the effect of BMP-2 release profile on the recruitment of bone marrow-derived osteoblast progenitor cells at the release site of BMP-2 and the consequent *de novo* generation of bone tissue.

Materials and Methods

Materials

A gelatin sample with an isoelectric point of 9.0 was isolated from the porcine skin by an acidic process of collagen (Nitta Gelatin, Osaka, Japan). $Na^{125}I$ (NEZ-033H, >12.95 GBq/mL) was purchased from Perkin-Elmer Life Sciences (Boston, MA). Other chemicals were obtained from Wako Pure Chemical Industries (Osaka, Japan) and used without further purification.

Preparation of gelatin hydrogels

Chemically crosslinked gelatin hydrogels with glutaraldehyde (GA) were prepared according to a previously reported method.[26] Briefly, aqueous solution of 3 wt% gelatin (pH 5.0) was mixed with GA at a final concentration of 0.16 and 0.09 wt%, respectively, followed by incubation at 4°C for 12 h for gelatin crosslinking. The gelatin hydrogel crosslinked was treated with 0.1 M glycine solution to block the residual aldehyde groups. After washing with double-distilled water for three times, the hydrogels were freeze-dried. The crosslinking extent of prepared hydrogels was evaluated by measuring the water content according to a previously described method.[27] The water contents of hydrogels prepared with higher and lower GA concentrations were 97.5 ± 0.1 and 99.3 ± 0.0 wt%, respectively.

In vivo *release test of BMP-2 from gelatin hydrogels*

All the animal experiments were performed according to the Institutional Guidance of Kyoto University on Animal Experimentation and with permission from the Animal Experiment Committee of the Institute for Frontier Medical Science, Kyoto University. All the surgical procedures were performed under continuous inhalation anesthesia using isoflurane (Forane®; Abbott Japan, Osaka, Japan) with 400 Anesthesia Unit (Univentor, Zejtun, Malta).

Human recombinant BMP-2 (Yamanouchi Pharmaceutical, Tokyo, Japan) was radioiodinated through the conventional chloramine T method as previously described.[28] Briefly, 5 μL of $Na^{125}I$ was added to 200 μL of BMP-2 solution (150 μg/mL) in 0.5 M potassium phosphate buffer (pH 7.5) containing 0.5 M sodium chloride. Then, 0.2 mg/mL of chloramine-T in the same buffer (100 μL) was added to the solution mixture. After agitation at room temperature for 2 min, 100 μL of phosphate-buffered saline (PBS; pH 7.4) containing 0.4 mg of sodium metabisulfate was added to the reaction solution to stop radioiodination. The reaction mixture was passed through a PD-10 desalting column (GE Healthcare Life Sciences, Giles, UK) to remove the uncoupled, free ^{125}I molecules from the ^{125}I-labeled BMP-2 (9.0 μg/mL; removal ratio of free ^{125}I = 97.0%).

PBS containing ^{125}I-labeled BMP-2 (27.4 μL, 9.0 μg/mL) and PBS containing nonlabeled BMP-2 (2.6 μL, 1 mg/mL) were mixed and dropped onto 2 mg of freeze-dried gelatin hydrogels, followed by incubation at 4°C for 12 h, to allow to swell into the hydrogel. Following the implantation of gelatin hydrogels incorporating ^{125}I-labeled BMP-2 into the back subcutis of 6-week-old, female ddY mice (18–20 g body weight; Shimizu Laboratory Supply, Kyoto, Japan), tissue around the implanted site was extracted at different time intervals after hydrogel implantation, and the tissue radioactivity was counted by a gamma counter to estimate the *in vivo* time profiles of BMP-2 release ($n = 3$, at each time point).

Preparation of green fluorescent protein-chimeric mice

C57BL/6 transgenic mice that ubiquitously express enhanced green fluorescent protein (GFP) under the Cyto-Megalovirus (CMV) early enhancer/chicken β actin (CAG) promoter were provided by RIKEN BRC through the National Bio-Resource Project of the MEXT, Japan. Preparation of chimeric mice was performed according to a previously reported procedure.[29] Briefly, bone marrow cells were isolated from 8- to 10-week-old, male transgenic mice under sterile conditions.[30] The cells were incubated with CD90.2 microbeads (no. 130-049-101; Miltenyi Biotec, Auburn, CA) and RPMI 1640 medium at 8°C for 20 min and passed through large depletion (LD) column with Midi MACS system (no. 130-042-901; Miltenyi Biotec) for depletion of CD-90.2-positive T cells and prevention of subsequent autoimmune attack. Eight- to 10-week-old, female C57BL/6 mice were irradiated lethally with 10 Gy of gamma ray. For total bone marrow transplantation, 5×10^6 of bone marrow cells prepared from GFP transgenic mice was intravenously administered to recipient irradiated mice. After the transplantation, the mice were bred for 10 weeks to complete the replacement of bone marrow cells to GFP-positive cells. The replacement ratio of bone marrow cells was 93.2% ± 1.5% when evaluated by the fluorescence-associated cell sorter method (FACS Calibur; BD Bioscience, Franklin Lakes, NJ).

In vivo *assay of* de novo *generation of bone tissue*

BMP-2 was dissolved in PBS at 100 μg/mL and the solution (30 μL) was dropped on the gelatin hydrogel (2 mg) to allow it to swell into the hydrogel. After incubation of the hydrogels incorporating BMP-2 at 4°C for 12 h, the hydrogels were implanted to the back subcutis of GFP-chimeric mice. As a control, gelatin hydrogels incorporating PBS were similarly implanted to the back of the mice. Then, the tissue around the implanted sites was extracted at different time intervals after hydrogel implantation, and the fluorescent images of tissues were obtained by a digital microscope (Multiviewer System VB-S20; Keyence, Osaka, Japan). *De novo* generation of bone tissue was radiologically exam-

ined by a soft X-ray machine (Hitex-100; Hitachi, Tokyo, Japan) at 54 kV and 2.5 mA for 20 s. Then the extracted tissues were fixed with 4% paraformaldehyde at 4°C for 48 h, and the bone tissue was decalcified with PBS containing 9 wt% ethylenediamine tetraacetic acid disodium salt and 10 wt% ethylenediamine tetraacetic acid tetrasodium salt (EDTA solution) at 4°C for 6 days. The EDTA solution was changed every other day. After decalcification, the pellets were equilibrated in PBS containing 15 wt% sucrose for 12 h and then in PBS containing 30 wt% sucrose for 12 h, embedded in Tissue-Tek OCT Compound (Sakura Finetek, Tokyo, Japan), frozen on dry ice, and stored at −80°C. For the histological examinations, 6-μm-thick sections were cut with a cryostat (Leica Microsystems AG, Wetzlar, Germany) at the portion of implanted site as central as possible, followed by staining with hematoxylin and eosin. The area of newly formed bone tissue was assessed in terms of histological image analysis using the computer program Image-Pro Plus 3.01 (Media-Cybernetics, Silver Spring, MD).

Immunofluorescence staining

After washing with PBS, the sections (6 μm thickness) were blocked with a normal goat serum for 1 h at room temperature before incubation with a rabbit polyclonal anti-mouse osteocalcin antibody (1:250; Takara Bio, Shiga, Japan) for 1 h at room temperature. Then the sections were stained with a tetramethylrhodamine-isothiocyanate-conjugated goat anti-rabbit IgG (Molecular Probes, Eugene, OR) for 1 h at room temperature. After washing with PBS, the sections were mounted with Vectashield® (Vector Laboratories, Burlingame, CA). Fluorescent images were obtained using an epifluorescent microscope (AX-80; Olympus, Tokyo, Japan), and the relative percentage number of GFP-positive cells to osteocalcin-positive cells in each image was calculated manually by observing the images. Three areas of interest ($100 \times 100\ \mu m^2$) were chosen randomly from each fluorescent image (at least four images per each experimental group) and the number of GFP- and osteocalcin-positive cells were counted.

In vitro *migration assay*

Bone marrow cells (3×10^6 cells/cm^2) isolated from the transgenic mice described earlier were plated onto cell culture dish (no. 430167; Corning Incorporated, Corning, NY) with alpha minimum essential medium (αMEM; Sigma-Aldrich, St. Louis, MO) containing 15 vol% fetal bovine serum (FBS) and cultured at 37°C and 5% CO_2–95% air atmospheric pressure. The cells were flushed with PBS at 3 days after seeding to remove unattached blood cells and cultured till subconfluent condition for further experiment. The medium was changed to αMEM without serum at 24 h before the migration assay experiment. The cells were trypsinized and plated onto the HTS® fluoroblok inserts (1.3×10^3 cells/mm^2; Falcon no. 351552 with 8-μm-diameter pore; Becton Dickinson, Franklin Lakes, NJ) with αMEM containing 0.5 vol% FBS. The bottom side of the inserts contacted αMEM containing 15 or 0.5 vol% FBS, 100 ng/mL of recombinant human stromal cell-derived factor-1 (SDF-1; no. 350-NS/CF; R&D systems, Minneapolis, MN), BMP-2, or recombinant human placental growth factor (PlGF; no. 264-PG; R&D systems) with 0.1 vol% bovine serum albumin. After 24 h culture, cells that migrated to the bottom side were counted from fluorescent photographs taken by an epifluorescent microscope (IX-70; Olympus). The number of cells in six images (0.594 mm^2 per each image) were counted.

Statistical analysis

All the results were statistically analyzed by the unpaired Student's *t*-test and $p < 0.05$ was considered to be statistically significant. Data were expressed as the mean ± standard deviation.

Results

De novo *generation of bone tissue by gelatin hydrogels incorporating BMP-2*

Figure 1 shows the time profiles of *in vivo* radioactivity remaining after implantation of gelatin hydrogels incorporating ^{125}I-labeled BMP-2 with different water contents. The gelatin hydrogels with higher water content released BMP-2 faster than those with lower water content.

Figure 2 shows the soft X-ray radiophotographs of implanted sites at 2 weeks after the implantation of gelatin hydrogels incorporating 3 μg of BMP-2 or PBS. A radio-opacity portion was observed at the center of tissues implanted with gelatin hydrogels incorporating BMP-2, although the influence of water content on the extent was not observed. On the contrary, no radio-opacity was observed for the BMP-2-free gelatin hydrogels.

Figure 3a–c shows the histological images of the implanted site at 2 weeks after implantation of the gelatin hydrogels incorporating 3 μg of BMP-2 or PBS. Figure 3d shows the histological image of the implanted site at 7 weeks after implantation of the gelatin hydrogel incorporating BMP-2.

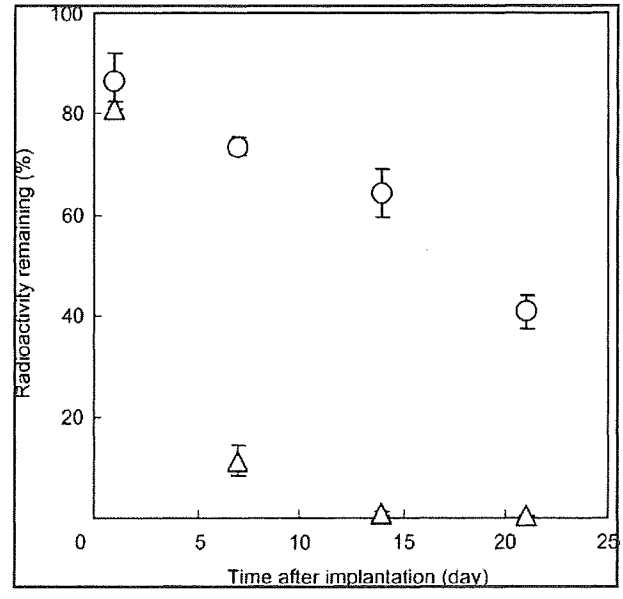

FIG. 1. *In vivo* release profiles of BMP-2 from gelatin hydrogels with water content of 97.5 wt% (○) and 99.3 wt% (Δ). BMP, bone morphogenetic protein.

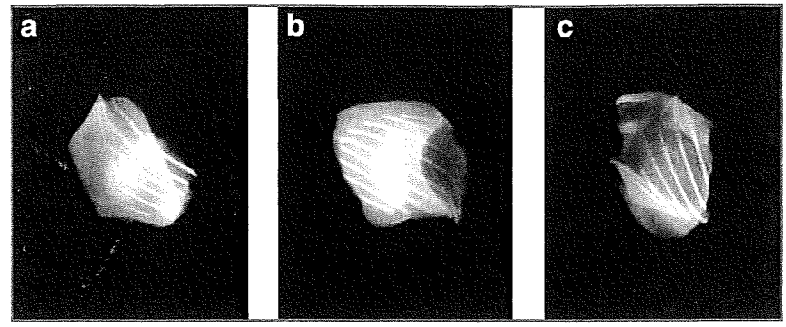

FIG. 2. Soft X-ray radiophotographs of tissues around the implanted site at 2 weeks after implantation of (a) the gelatin hydrogel incorporating BMP-2 (3 μg) with a water content of 97.5 wt%, (b) the gelatin hydrogel incorporating BMP-2 (3 μg) with a water content of 99.3 wt%, and (c) the gelatin hydrogel incorporating PBS with a water content of 97.3 wt%. PBS, phosphate-buffered saline.

After implantation, mature bone tissues with a bone marrow-like structure containing many inflammatory cells, blood cells, and adipocytes (Fig. 3e) were observed. The implanted gelatin hydrogel was completely degraded and was not detected in the section. Figure 4 shows the area of newly formed bone tissue at the implanted site of gelatin hydrogels incorporating BMP-2. After the implantation of gelatin hydrogel incorporating BMP-2 with a water content of 99.3 wt%, the *de novo* generation of bone tissue was observed only at 2 weeks, but thereafter the tissue disappeared. On the contrary, the implantation of hydrogels incorporating BMP-2 with a water content of 97.5 wt% induced significant *de novo* generation of bone tissue and the bone tissue was retained even at 7 weeks after implantation.

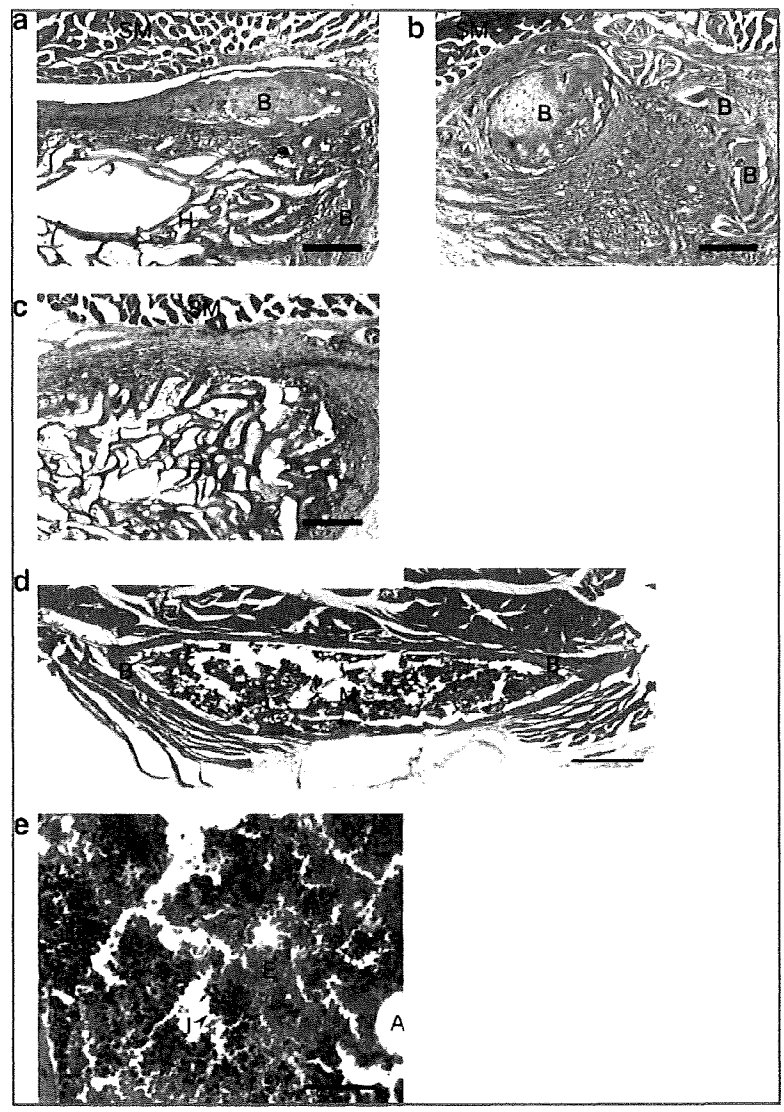

FIG. 3. (a–c) Histological image of tissues around the implanted site at 2 weeks after implantation of (a) the gelatin hydrogel incorporating BMP-2 (3 μg) with a water content of 97.5 wt%, (b) the gelatin hydrogel incorporating BMP-2 (3 μg) with a water content of 99.3 wt%, and (c) the gelatin hydrogel incorporating PBS with a water content of 97.5 wt%. B, bone tissue; M, bone marrow-like structure; SM, subcutaneous muscle tissue; H, remaining gelatin hydrogels. (d) Histological image of tissues around the implanted site at 7 weeks after implantation of gelatin hydrogel incorporating BMP-2 (3 μg) with a water content of 97.5 wt%. Scale bar = 500 μm. (e) Higher magnification image of bone marrow-like structure inside the implanted site. Scale bar = 50 μm. I, inflammatory cells; E, blood cells; A, adipocyte. Color images available online at www.liebertonline.com/ten.

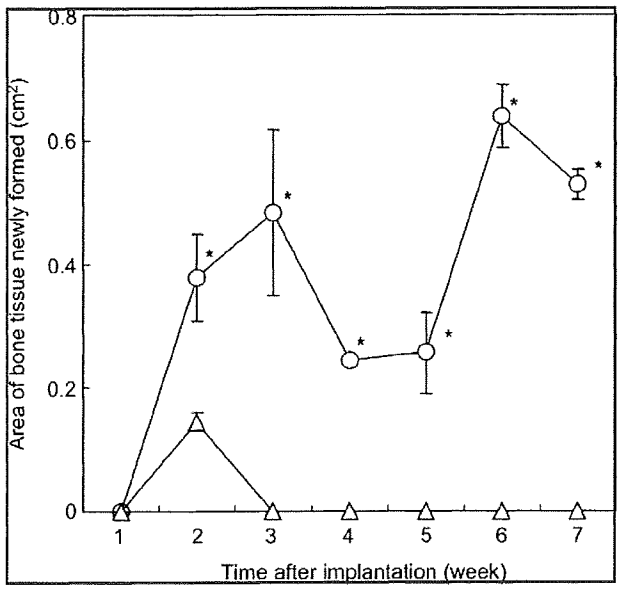

FIG. 4. Area of newly formed bone tissues after implantation of gelatin hydrogels incorporating BMP-2 (3 μg) with a water content of 97.5 wt% (○), gelatin hydrogels incorporating BMP-2 (3 μg) with a water content of 99.3 wt% (Δ). *$p < 0.05$, significant against the area after implantation of gelatin hydrogels incorporating BMP-2 (3 μg) with a water content of 99.3 wt% at the corresponding time.

Recruitment of cells by gelatin hydrogels incorporating BMP-2

Figure 5 shows the fluorescent images of tissues around the implanted site at 2 weeks after the implantation of gelatin hydrogels incorporating BMP-2 or PBS. Irrespective of the experimental groups, a green fluorescence was detected in the implanted sites, which indicates the accumulation of bone marrow-derived cells.

Figure 6 shows the immunofluorescent images of tissues around the implanted site at 2 weeks after implantation of gelatin hydrogels incorporating BMP-2 or PBS. Cells with green fluorescence were observed in all images, and the cells were of round and spindle shape. For the gelatin hydrogels incorporating BMP-2, many red-stained cells were observed around the implanted site (Fig. 6a, b). On the contrary, no cells with red fluorescence were observed around the implanted site of gelatin hydrogels without BMP-2 (Fig. 6c). Figure 7 shows the relative percentage number of GFP-positive cells to osteocalcin-positive cells around the implanted site at 2 weeks after implantation of gelatin hydrogels incorporating BMP-2 or PBS. The implantation of gelatin hydrogels incorporating BMP-2 with different water contents increased the relative percentage number of GFP-positive cells to osteocalcin-positive cells around the implanted site. And the relative percentage for the gelatin hydrogel incorporating BMP-2 with a water content of 97.5 wt% was significantly higher than that of hydrogels with a water content 99.3 wt%. After this time point, it was practically impossible to compare the accumulation of bone marrow-derived cells between the implanted sites of the gelatin hydrogel incorporating BMP-2 with water contents of 97.5 and 99.3 wt%. This is due to the disappearance of the newly formed bone tissue around the implanted site of the latter gelatin hydrogel incorporating BMP-2.

In vitro *cell migration*

Figure 8 shows the number of cells that migrated to the bottom side of the inserts at 24 h after incubation with αMEM containing BMP-2 or other factors. No activity as a chemoattractant to bone marrow cells was observed for BMP-2. The migration level was the same as that of the negative control (0.5 vol% FBS). However, a strong chemoattractant activity was observed for SDF-1 and PlGF, which was the same as that of the positive control (15 vol% FBS). The activity by PlGF was significantly higher than that by SDF-1 and 15 vol% FBS.

Discussion

This study demonstrates that the BMP-2 release profile affected the extent of accumulation of bone marrow-derived cells and the consequent *de novo* generation of bone tissues. The hydrogel water contents of 97.5 and 99.3 wt% indicated that the weight ratio of gelatin molecules to total hydrogel were 2.5 and 0.7 wt%. The difference in gelatin molecule fraction and crosslinking density of hydrogels caused the difference in hydrogel degradation and the consequent BMP-2 *in vivo* release profiles (Fig. 1). The BMP-2 release for a longer time period enabled strong accumulation of GFP-positive bone marrow-derived osteoblast progenitor cells which are also stained with the anti-osteocalcin antibody, even at 2 weeks after implantation. It is apparent from Figure 5 that the accumulation of bone marrow-derived cells was observed by the implantation of gelatin hydrogels with or without BMP-2. However, from the double-staining assay, for the hydrogel without BMP-2, no osteocalcin-positive cells were detected around the implanted site (Figs. 6 and 7). As

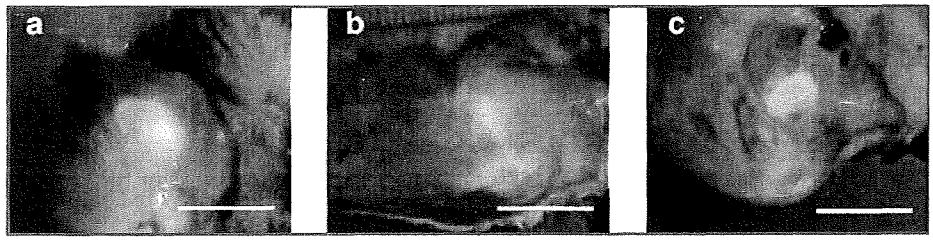

FIG. 5. Fluorescent images of the area surrounding the implant at 2 weeks after implantation of (**a**) the gelatin hydrogel incorporating BMP-2 (3 μg) with a water content of 97.5 wt%, (**b**) the gelatin hydrogel incorporating BMP-2 (3 μg) with a water content of 99.3 wt%, and (**c**) the gelatin hydrogel incorporating PBS with a water content of 97.3 wt%. Scale bar = 1 cm. Color images available online at www.liebertonline.com/ten.

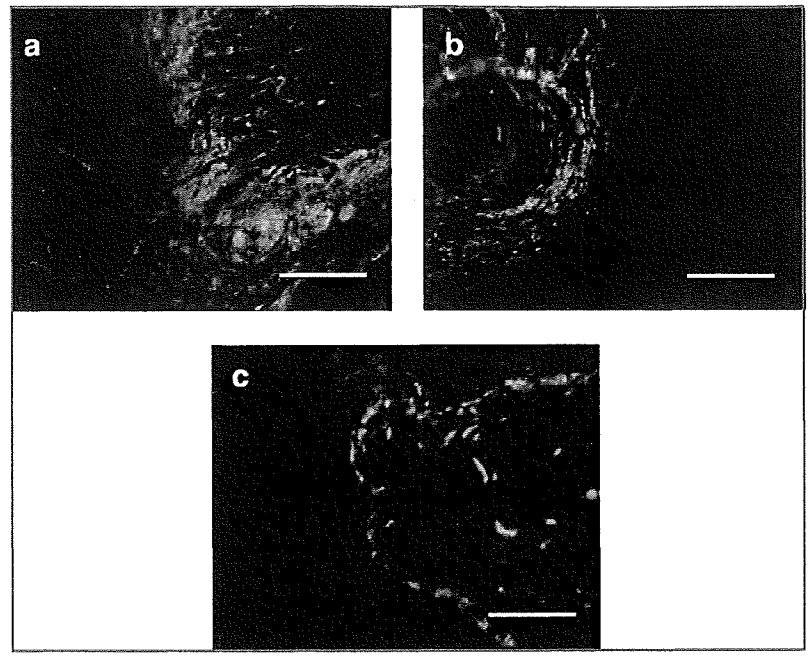

FIG. 6. Immunofluorescence staining images of tissue around the implanted site at 2 weeks after implantation of (a) the gelatin hydrogel incorporating BMP-2 (3 μg) with a water content of 97.5 wt%, (b) the gelatin hydrogel incorporating BMP-2 (3 μg) with a water content of 99.3 wt%, and (c) the gelatin hydrogel incorporating PBS with a water content of 97.3 wt%. Red fluorescence: osteocalcin; green fluorescence: green fluorescent protein. Scale bar = 200 μm. Color images available online at www.liebertonline.com/ten.

the osteocalcin-expressing cells are generally osteoblastic cells with bone formation activity, we can say with certainty that the BMP-2 release increased the recruitment of osteogenic cells around the release site.

The extent of *de novo* generation of bone tissue depended on the water content of gelatin hydrogels. This finding was experimentally confirmed in a previous study[26] and the present results are also in accordance to it even after extended time course (7 weeks after implantation). The decrease in the *de novo* generated area was observed in 4 or 5 and 3 weeks after implantation for gelatin hydrogels with water contents of 97.5 and 99.3 wt%, respectively (Fig. 4). This time profile can be explained in terms of that of BMP-2 release. For the gelatin hydrogel, the time profile of BMP-2 release was well correlated to that of hydrogel degradation. The hydrogel that is degraded for 4–5 weeks would release

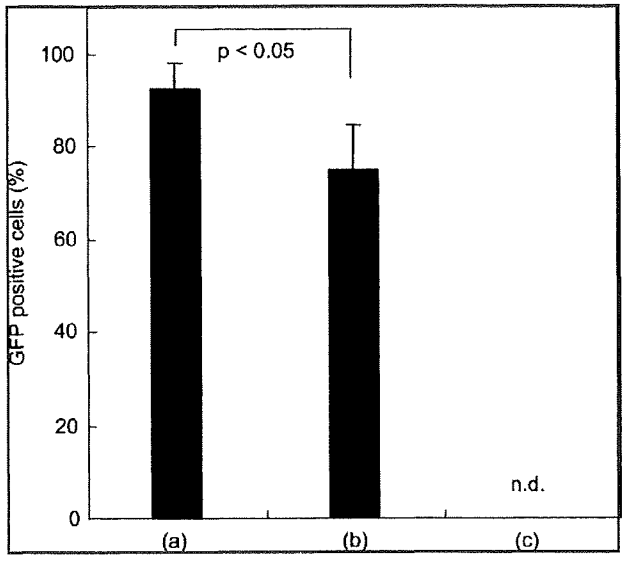

FIG. 7. Relative percentage number of GFP-positive cells to osteocalcin-positive cells around the implanted site at 2 weeks after implantation of (a) gelatin hydrogels incorporating BMP-2 (3 μg) with a water content of 97.5 wt%, (b) gelatin hydrogels incorporating BMP-2 (3 μg) with a water content of 99.3 wt%, and (c) gelatin hydrogels incorporating PBS with a water content of 97.5 wt%. n.d., not detected; GFP, green fluorescent protein.

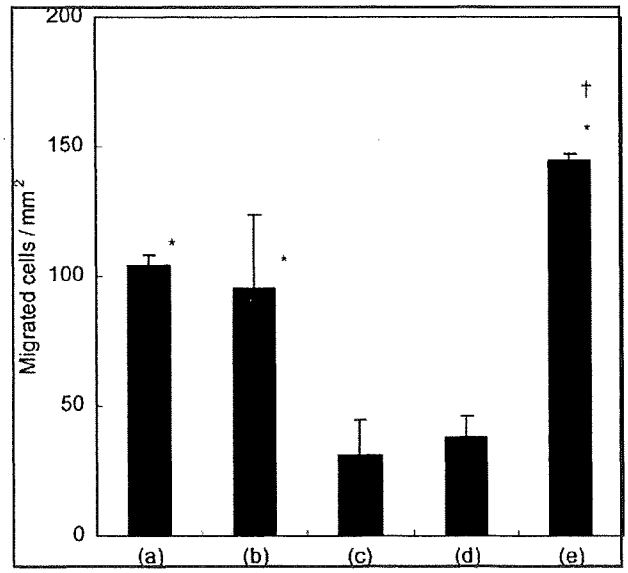

FIG. 8. Migration of bone marrow cells through the transwell membrane at 24 h after incubation with α-minimum essential medium containing (a) 15 vol% fetal bovine serum, (b) 100 ng/mL stromal cell-derived factor-1, (c) 100 ng/mL BMP-2, (d) 0.5 vol% fetal bovine serum, and (e) 100 ng/mL placental growth factor. $^{*}p < 0.05$ against the groups (c) and (d); $^{\dagger}p < 0.05$ significant against the groups (a) and (b).

BMP-2 for 4–5 weeks. It is possible that for this range, the BMP-2 release results in the BMP-induced *de novo* generation of bone tissue. However, the cessation of release would suppress bone tissue induction, resulting in the disappearance of bone tissue. The area of *de novo* generated bone increased again from 6 weeks after implantation. The cells recruited by the released and remaining BMP-2 may be able to further promote *de novo* generation of bone tissue. This reason is not clear at present.

Significant difference in the accumulation of osteocalcin-positive cells between the gelatin hydrogels with water contents of 97.5 and 99.3 wt% was observed (Fig. 6). This experimental result indicates that the profile of BMP-2 release affects the recruitment of bone marrow-derived cells. It is conceivable that BMP-2 release for a longer time period induces the recruitment of cells for a long time period, resulting in enhanced accumulation of cells. BMP-2 can accelerate bone tissue formation[18] through osteoblast migration,[31] by promoting osteogenic differentiation of mesenchymal stem cells,[32,33] angiogenesis,[34] apoptosis of osteoblast,[35] and recruitment of osteoblast progenitor cells.[21,29] It has been demonstrated that BMP-2 could induce the expression of PlGF. The enhanced expression of PlGF promoted the recruitment of progenitor cells from the bone marrow.[36–38] In addition, fibrous tissue and hypertrophic cartilage formation was observed in a fracture healing model of PlGF-deficient mice.[37] The chemoattractant study revealed that PlGF accelerated the migration of isolated bone marrow cells, in contrast to BMP-2 (Fig. 8). It is highly conceivable that BMP-2 functions as a trigger molecule to induce PlGF for the migration of bone marrow-derived cells. Further analysis is needed to understand the effect of BMP-2 release on cell recruitment.

This study clearly indicates that the BMP-2-releasing materials enhance cell accumulation for *de novo* generation of bone tissue. This activity could be modified by the release profile. This finding opens a new strategy of tissue engineering to achieve tissue regeneration by induction of cells present in the body.

Disclosure Statement

No competing financial interests exist.

References

1. Langer, R. Tissue engineering: perspectives, challenges, and future directions. Tissue Eng **13,** 1, 2007.
2. Morrison, S.J., and Spradling, A.C. Stem cells and niches: mechanisms that promote stem cell maintenance throughout life. Cell **132,** 598, 2008.
3. Ingber, D.E., Mow, V.C., Butler, D., Niklason, L., Huard, J., Mao, J., Yannas, I., Kaplan, D., and Vunjak-Novakovic, G. Tissue engineering and developmental biology: going biomimetic. Tissue Eng **12,** 3265, 2006.
4. Matsumoto, T., and Mooney, D.J. Cell instructive polymers. Adv Biochem Eng Biotechnol **102,** 113, 2006.
5. Badylak, S.F. The extracellular matrix as a biologic scaffold material. Biomaterials **28,** 3587, 2007.
6. Ceradini, D.J., Kulkarni, A.R., Callaghan, M.J., Tepper, O.M., Bastidas, N., Kleinman, M.E., Capla, J.M., Galiano, R.D., Levine, J.P., and Gurtner, G.C. Progenitor cell trafficking is regulated by hypoxic gradients through HIF-1 induction of SDF-1. Nat Med **10,** 858, 2004.
7. Eghbali-Fatourechi, G.Z., Lamsam, J., Fraser, D., Nagel, D., Riggs, B.L., and Khosla, S. Circulating osteoblast-lineage cells in humans. N Engl J Med **352,** 1959, 2005.
8. Grunewald, M., Avraham, I., Dor, Y., Bachar-Lustig, E., Itin, A., Yung, S., Chimenti, S., Landsman, L., Abramovitch, R., and Keshet, E. VEGF-induced adult neovascularization: recruitment, retention, and role of accessory cells. Cell **124,** 175, 2006.
9. Jin, D.K., Shido, K., Kopp, H.G., Petit, I., Shmelkov, S.V., Young, L.M., Hooper, A.T., Amano, H., Avecilla, S.T., Heissig, B., Hattori, K., Zhang, F., Hicklin, D.J., Wu, Y., Zhu, Z., Dunn, A., Salari, H., Werb, Z., Hackett, N.R., Crystal, R.G., Lyden, D., and Rafii, S. Cytokine-mediated deployment of SDF-1 induces revascularization through recruitment of $CXCR4^{+}$ hemangiocytes. Nat Med **12,** 557, 2006.
10. Karp, J.M., and Leng Teo, G.S. Mesenchymal stem cell homing: the devil is in the details. Cell Stem Cell **4,** 206, 2009.
11. Kuznetsov, S.A., Mankani, M.H., Gronthos, S., Satomura, K., Bianco, P., and Robey, P.G. Circulating skeletal stem cells. J Cell Biol **153,** 1133, 2001.
12. Wan, C., He, Q., and Li, G. Allogenic peripheral blood derived mesenchymal stem cells (MSCs) enhance bone regeneration in rabbit ulna critical-sized bone defect model. J Orthop Res **24,** 610, 2006.
13. Wragg, A., Mellad, J.A., Beltran, L.E., Konoplyannikov, M., San, H., Boozer, S., Deans, R.J., Mathur, A., Lederman, R.J., Kovacic, J.C., and Boehm, M. VEGFR1/CXCR4-positive progenitor cells modulate local inflammation and augment tissue perfusion by a SDF-1-dependent mechanism. J Mol Med **86,** 1221, 2008.
14. Zhou, B., Han, Z.C., Poon, M.C., and Pu, W. Mesenchymal stem/stromal cells (MSC) transfected with stromal derived factor 1 (SDF-1) for therapeutic neovascularization: enhancement of cell recruitment and entrapment. Med Hypotheses **68,** 1268, 2007.
15. Zhu, W., Boachie-Adjei, O., Rawlins, B.A., Frenkel, B., Boskey, A.L., Ivashkiv, L.B., and Blobel, C.P. A novel regulatory role for stromal-derived factor-1 signaling in bone morphogenic protein-2 osteogenic differentiation of mesenchymal C2C12 cells. J Biol Chem **282,** 18676, 2007.
16. Tabata, Y. Significance of release technology in tissue engineering. Drug Discov Today **10,** 1639, 2005.
17. Reddi, A.H. Bone morphogenetic proteins: from basic science to clinical applications. J Bone Joint Surg Am **83-A Suppl 1,** S1, 2001.
18. Wozney, J.M. Overview of bone morphogenetic proteins. Spine **27,** S2, 2002.
19. Wozney, J.M., Rosen, V., Celeste, A.J., Mitsock, L.M., Whitters, M.J., Kriz, R.W., Hewick, R.M., and Wang, E.A. Novel regulators of bone formation: molecular clones and activities. Science **242,** 1528, 1988.
20. Bessa, P.C., Casal, M., and Reis, R.L. Bone morphogenetic proteins in tissue engineering: the road from laboratory to clinic, part II (BMP delivery). J Tissue Eng Regen Med **2,** 81, 2008.
21. Otsuru, S., Tamai, K., Yamazaki, T., Yoshikawa, H., and Kaneda, Y. Bone marrow-derived osteoblast progenitor cells in circulating blood contribute to ectopic bone formation in mice. Biochem Biophys Res Commun **354,** 453, 2007.
22. Bruder, S.P., Fink, D.J., and Caplan, A.I. Mesenchymal stem cells in bone development, bone repair, and skeletal regeneration therapy. J Cell Biochem **56,** 283, 1994.
23. Colnot, C., Huang, S., and Helms, J. Analyzing the cellular contribution of bone marrow to fracture healing using bone marrow transplantation in mice. Biochem Biophys Res Commun **350,** 557, 2006.

24. Ozaki, A., Tsunoda, M., Kinoshita, S., and Saura, R. Role of fracture hematoma and periosteum during fracture healing in rats: interaction of fracture hematoma and the periosteum in the initial step of the healing process. J Orthop Sci **5,** 64, 2000.
25. Utvag, S.E., Grundnes, O., and Reikeras, O. Effects of degrees of reaming on healing of segmental fractures in rats. J Orthop Trauma **12,** 192, 1998.
26. Yamamoto, M., Takahashi, Y., and Tabata, Y. Controlled release by biodegradable hydrogyels enhances the ectopic bone formation of bone morphogenetic protein. Biomaterials **24,** 4375, 2003.
27. Tabata, Y., Nagano, A., Muniruzzaman, M., and Ikada, Y. *In vitro* sorption and desorption of basic fibroblast growth factor from biodegradable hydrogels. Biomaterials **19,** 1781, 1998.
28. Ozeki, M., and Tabata, Y. *In vivo* degradability of hydrogels prepared from different gelatins by various cross-linking methods. J Biomater Sci Polym Ed **16,** 549, 2005.
29. Otsuru, S., Tamai, K., Yamazaki, T., Yoshikawa, H., and Kaneda, Y. Circulating bone marrow-derived osteoblast progenitor cells are recruited to the bone-forming site by the CXCR4/stromal cell-derived factor-1 pathway. Stem Cells **26,** 223, 2008.
30. Okabe, M., Ikawa, M., Kominami, K., Nakanishi, T., and Nishimune, Y. Green mice as a source of ubiquitous green cells. FEBS Lett **407,** 313, 1997.
31. Sotobori, T., Ueda, T., Myoui, A., Yoshioka, K., Nakasaki, M., Yoshikawa, H., and Itoh, K. Bone morphogenetic protein-2 promotes the haptotactic migration of murine osteoblastic and osteosarcoma cells by enhancing incorporation of integrin beta1 into lipid rafts. Exp Cell Res **312,** 3927, 2006.
32. Wagner, T.U. Bone morphogenetic protein signaling in stem cells—one signal, many consequences. FEBS J **274,** 2968, 2007.
33. Bessa, P.C., Pedro, A.J., Klosch, B., Nobre, A., van Griensven, M., Reis, R.L., and Casal, M. Osteoinduction in human fat-derived stem cells by recombinant human bone morphogenetic protein-2 produced in *Escherichia coli.* Biotechnol Lett **30,** 15, 2008.
34. Deckers, M.M., van Bezooijen, R.L., van der Horst, G., Hoogendam, J., van Der Bent, C., Papapoulos, S.E., and Lowik, C.W. Bone morphogenetic proteins stimulate angiogenesis through osteoblast-derived vascular endothelial growth factor A. Endocrinology **143,** 1545, 2002.
35. Hay, E., Lemonnier, J., Fromigue, O., and Marie, P.J. Bone morphogenetic protein-2 promotes osteoblast apoptosis through a Smad-independent, protein kinase C-dependent signaling pathway. J Biol Chem **276,** 29028, 2001.
36. Marrony, S., Bassilana, F., Seuwen, K., and Keller, H. Bone morphogenetic protein 2 induces placental growth factor in mesenchymal stem cells. Bone **33,** 426, 2003.
37. Maes, C., Coenegrachts, L., Stockmans, I., Daci, E., Luttun, A., Petryk, A., Gopalakrishnan, R., Moermans, K., Smets, N., Verfaillie, C.M., Carmeliet, P., Bouillon, R., and Carmeliet, G. Placental growth factor mediates mesenchymal cell development, cartilage turnover, and bone remodeling during fracture repair. J Clin Invest **116,** 1230, 2006.
38. Fiedler, J., Leucht, F., Waltenberger, J., Dehio, C., and Brenner, R.E. VEGF-A and PlGF-1 stimulate chemotactic migration of human mesenchymal progenitor cells. Biochem Biophys Res Commun **334,** 561, 2005.

Address correspondence to:
Yasuhiko Tabata, Ph.D., D.Med.Sci., D.Pharm.
Department of Biomaterials
Institute for Frontier Medical Sciences
Kyoto University
53 Kawara-cho Shogoin
Sakyo-ku
Kyoto 6068507
Japan

E-mail: yasuhiko@frontier.kyoto-u.ac.jp

Received: May 13, 2009
Accepted: November 3, 2009
Online Publication Date: December 15, 2009

Diagnosis and Treatment of Stevens-Johnson Syndrome and Toxic Epidermal Necrolysis with Ocular Complications

Chie Sotozono, MD, PhD,[1] Mayumi Ueta, MD, PhD,[1] Noriko Koizumi, MD, PhD,[1] Tsutomu Inatomi, MD, PhD,[1] Yuji Shirakata, MD, PhD,[2] Zenro Ikezawa, MD, PhD,[3] Koji Hashimoto, MD, PhD,[2] Shigeru Kinoshita, MD, PhD[1]

Purpose: To present a detailed clarification of the symptoms at disease onset of Stevens-Johnson syndrome (SJS) and its more severe variant, toxic epidermal necrolysis (TEN), with ocular complications and to clarify the relationship between topical steroid use and visual prognosis.

Design: Cross-sectional study.

Participants: Ninety-four patients with SJS and TEN with ocular complications.

Methods: A structured interview, examination of the patient medical records, or both addressing clinical manifestations at disease onset were conducted for 94 patients seen at Kyoto Prefectural University of Medicine. Any topical steroid use during the first week at the acute stage also was investigated.

Main Outcome Measures: The incidence and the details of prodromal symptoms and the mucosal involvements and the relationship between topical steroid use and visual outcomes.

Results: Common cold-like symptoms (general malaise, fever, sore throat, etc.) preceded skin eruptions in 75 cases, and extremely high fever accompanied disease onset in 86 cases. Acute conjunctivitis and oral and nail involvements were reported in all patients who remembered the details. Acute conjunctivitis occurred before the skin eruptions in 42 patients and simultaneously in 21 patients, whereas only 1 patient reported posteruption conjunctivitis. Visual outcomes were significantly better in the group receiving topical steroids compared with those of the no-treatment group ($P<0.00001$).

Conclusions: Acute conjunctivitis occurring before or simultaneously with skin eruptions accompanied by extremely high fever and oral and nail involvement indicate the initiation of SJS or TEN. Topical steroid treatment from disease onset seems to be important for the improvement of visual prognosis.

Financial Disclosure(s): The author(s) have no proprietary or commercial interest in any materials discussed in this article. *Ophthalmology 2009;116:685–690 © 2009 by the American Academy of Ophthalmology.*

Stevens-Johnson syndrome (SJS) and its more severe variant, toxic epidermal necrolysis (TEN), are acute inflammatory disorders that affect the skin and mucous membranes.[1–4] Although the incidence of SJS and TEN is very low, approximately 0.4 to 1 case per 1 million persons and 1 to 6 cases per 1 million persons, respectively, both can affect anybody at any age, usually as a consequence of adverse drug reactions.[5–7] A variety of drugs including antibiotics, nonsteroidal anti-inflammatory drugs, and antiepileptic medications, that is, any of the popularly used drugs, have been reported to cause severe drug reactions and to induce SJS or TEN.

The mortality rates for SJS and TEN are high: 1% to 5% and 25% to 35%, respectively.[8,9] Ocular complications occur in more than 50% of the patients, and ocular surface inflammation develops rapidly at the acute stage.[10,11] Extensive inflammation of the ocular surface often is accompanied by pseudomembranous formation and corneal or conjunctival epithelial defects, or both. The common pathway after the acute stage includes persistent epithelial defects, ulceration, and perforation, finally developing into corneal cicatricial changes such as neovascularization, opacification, keratinization, and symblepharon.[12,13] Even after the acute-stage impairments subside, permanent visual impairment or blindness remains and conjunctival inflammation prolongs at the chronic stage.[14] Patients with SJS or TEN require life-long management for ocular discomfort and morbidity. Stevens-Johnson syndrome or TEN accompanied by ocular complications, at both the acute and chronic stage, are 2 of the most devastating ocular surface diseases, and both are extremely difficult to treat.

The loss of corneal epithelial stem cells, which are located in the limbal region,[15–18] evidenced by the loss of palisades of Vogt, is the most common ocular feature of SJS.[13] As soon as the corneal epithelial stem cells are lost at the acute stage of SJS or TEN, the corneal epithelium does not regenerate, thus resulting in conjunctival epithelial invasion into the cornea (conjunctivalization) and cicatricial changes of the ocular surface. In contrast, the regeneration of the epidermis develops rather smoothly at the remission of the diseases.

Penetrating keratoplasty (PK) generally is contraindicated for eyes with SJS or TEN because PK does not supply the limbal region of the eye with corneal epithelial stem

ISSN 0161-6420/09/$–see front matter
doi:10.1016/j.ophtha.2008.12.048

cells. Moreover, PK-initiated, immunologically driven ocular surface inflammation may induce persistent epithelial defects and corneal melting, perforation, or both, ultimately resulting in blindness.[12] Allograft transplantation of healthy limbal tissue is useful for the reconstruction of the ocular surface. However, long-term outcomes are poor in eyes with SJS or TEN.[19] Groundbreaking surgical procedures have been developed over the past 12 years. We first reported the usefulness of cultivated corneal epithelial transplantation for SJS with persistent epithelial defects after the acute stage.[20–23] In another report, we clarified the efficacy of ex vivo expanded autologous oral mucosal epithelial cells to the ocular surface.[24] Cultivated oral mucosal epithelial transplantation and the 2-step surgical combination of cultivated oral mucosal epithelial transplantation and PK have provided the patients with SJS or TEN with a surgical pathway toward restoration of their visual function.[25–27] However, it is impossible for the ocular surface of those patients to be restored to its previously normal state.

Diagnosis of SJS or TEN at disease onset is complex, often confusing, and very difficult. Moreover, the use of steroids for treatment remains controversial.[10,28–30] Our recent reports and those of others indicated the influence of genetic endowment in SJS and TEN.[31–40] For instance, there are statistically significant differences in single nucleotide polymorphisms of toll-like receptor 3, interleukin (IL)-4R/IL-13, and Fas ligand in SJS and TEN; thus, genetic screening may help to deliver a more rapid diagnosis in the future. At present, however, the understanding of the typical clinical picture of SJS and TEN is still a vital aspect of early diagnosis and the initiation of treatment. Therefore, this study investigated the clinical manifestation at disease onset of SJS and TEN with ocular complications and evaluated the relationship between ophthalmic management at the acute stage and the visual outcomes.

Patients and Methods

From November 2005 through May 2008, extensive interviews were conducted with 94 patients (45 males and 49 females) with SJS or TEN with ocular complications seen at the SJS outpatient service at Kyoto Prefectural University Hospital. Of those patients, 88 cases were referral patients from the greater Japan area who had come to the SJS service at the acute stage (n = 14) or at the chronic stage (n = 74). Their ages ranged from 1 to 83 years (mean age±standard deviation, 41.6±18.5 years). At disease onset, the patients' ages ranged from 0 to 77 years (mean age±standard deviation, 26.2±18.8 years), and the duration of the illness ranged from 1 to 48 years (mean±standard deviation, 16.1±15.2 years). The questionnaires used in this study were structured as follows: (1) age of the patient at disease onset; (2) causative drugs; (3) the presence of prodromal symptoms; and (4) the episodes of high fever, conjunctivitis, skin eruptions, fingernail loss, and associated mucous membrane involvements. Medical records also were examined or the patients were asked directly regarding any ophthalmic management, especially the use of topical steroids, during the first week from disease onset. Then, the Mann–Whitney *U* test was used to analyze the correlation between the use of topical steroids and the visual outcomes. This study was approved by the Institutional Review Board of Kyoto Prefectural University of Medicine, Kyoto, Japan.

The diagnosis of SJS or TEN at the acute stage was based on the acute onset of high fever, serious mucocutaneous illness with skin eruptions, involvement of at least 2 mucosal sites, and the pathologic findings of a skin biopsy that demonstrated necrotic changes of the dermis. The diagnosis of SJS or TEN at the chronic stage was based on ocular cicatricial findings such as symblepharon, severe dry eye, corneal neovascularization, opacification, and conjunctivalization, and a confirmed history of the acute onset of high fever, serious mucocutaneous illness with skin eruptions, and involvement of at least 2 mucosal sites including the ocular surface. In the patients where disease onset occurred before age 10 years or in those who had lost consciousness at the acute stage because the illness, specific details were obtained by directly interviewing members of the immediate family.

Results

Of the 94 patients, drugs were the most commonly associated etiologic factor in 84 patients (89.4%). The causative drugs were cold remedies in 30 patients, antibiotics in 23 patients, nonsteroidal anti-inflammatory drugs in 19 patients, anticonvulsants in 5 patients, and others (anticancer agents, antirheumatic drugs, antimalarial, Chinese medicine, etc.).

Best-corrected visual acuity obtained at the chronic stage was 20/20 or better in 34 eyes (18.3%; Fig 1A), worse than 20/20 and up to and including 20/200 in 55 eyes (29.6%; Fig 1B), worse than 20/200 and up to and including 20/2000 in 53 eyes (28.5%; Fig 1C), and worse than 20/2000 in 44 eyes (23.7%; Fig 1D). Two eyes of 1 boy who was 1 year or age were excluded from the results because his visual acuity could not be assessed.

Characteristics of Stevens-Johnson Syndrome and Toxic Epidermal Necrolysis with Ocular Complications

Of the 94 patients, common coldlike symptoms (general malaise, fever, sore throat, etc.) preceded skin eruptions in 75 patients. Extremely high fever (more than 39° C) was reported by 86 patients, whereas 1 patient reported no fever and the remaining 7 patients could not remember the extent of the fever. Acute conjunctivitis and oral involvements (blisters, erosions, and bleeding of the mouth and lips) occurred in all patients who could recollect their symptoms in detail. Fingernail loss at the acute stage or deformation at present existed in all patients (Table 1; Fig 2). Other mucous membrane involvements included those of the pharynx, respiratory tract, or ear canal.

Forty-two patients reported episodes of acute conjunctivitis several hours to 4 days before the skin eruptions, and 21 patients reported that skin eruptions and conjunctivitis occurred simultaneously. Only 1 patient reported posteruption conjunctivitis (Table 2).

Topical Steroid Instillation and Visual Outcomes

Thirty-three patients (13 males and 20 females; mean age±standard deviation at disease onset, 31.5±18.6 years) began topical steroid treatment during the first week from disease onset, whereas 31 patients (14 males and 17 females; mean age±standard deviation, 27.9±19.5 years) received no topical steroid treatment or any other treatment for their eyes. The remaining 30 patients could not recall the details of ocular management during the first week from disease onset. Visual outcomes were significantly better in the group that received topical steroids at the acute stage compared with those of the no-treatment group ($P<0.00001$; Fig 3).

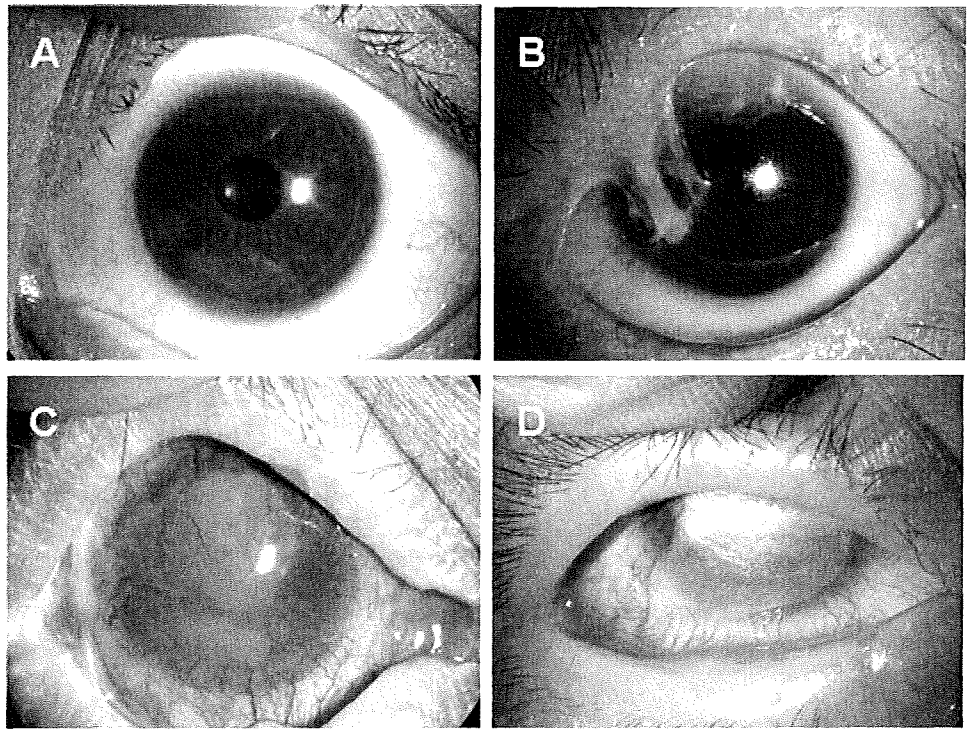

Figure 1. Photographs showing representative ocular manifestations at the chronic stage, with corresponding visual acuity. A, Clear cornea and best-corrected visual acuity of 20/20 or better: 34 eyes (18.3%). B, Moderate conjunctivalization and visual acuity worse than 20/20 and up to and including 20/200: 55 eyes (29.6%). C, Severe conjunctivalization and neovascularization and visual acuity worse than 20/200 and up to and including 20/2000: 53 eyes (28.5%). D, Keratinization, severe opacification, and visual acuity worse than 20/2000: 44 eyes (23.7%).

Diagnosis at the Acute Stage

Eleven patients were diagnosed with acute conjunctivitis by ophthalmologists before the development of systemic eruptions. An additional 12 patients were misdiagnosed as having measles (n = 4), chickenpox (n = 2), herpetic infection (n = 2), rubella (n = 1), or other diseases by physicians in other fields.

Among 94 patients, only 37 patients were diagnosed as having SJS or TEN at disease onset. Seven patients were diagnosed properly at several weeks (range, 2–8 weeks) after the onset, and surprisingly, 6 patients obtained the diagnosis at 2 to 45 years after the onset. For the remaining patients, when they received a proper diagnosis could not be ascertained.

Table 1. Symptoms and Mucosal Involvements of the 94 Patients at the Acute Stage

Symptoms	Experienced	Did Not Experience	Unknown
Prodromal common cold-like symptoms	75	17	2
Extremely high fever (>39° C)	86	1	7
Ocular involvement	94	0	0
Oral involvement	82	0	12
Genital involvement	46	18	30
Fingernail loss or deformation	94	0	0

Discussion

Stevens-Johnson syndrome and TEN are rare but potentially fatal skin disorders. Ocular involvement is common and often results in long-term complications such as serious visual impairment with ocular discomforts.[13,28] Although much has been learned over the past 50 years about the management of SJS and TEN, the following 3 important problems still remain: (1) the difficulty of obtaining a prompt and accurate diagnosis of SJS or TEN at disease onset, (2) ocular involvement often is overlooked easily because of the serious general symptoms and high lethality of these 2 diseases, and (3) a universally accepted treatment regimen for SJS and TEN has yet to be adopted and treatment with corticosteroids remains controversial.[10,28–30] There is also no standardized ophthalmologic treatment for the prevention of ocular complications.

In this study, 12 patients were misdiagnosed as having chickenpox, measles, herpetic infection, or other diseases. For early diagnosis, the clinical pictures of SJS and TEN need to be well understood, and to that end, the results of this study provided new and important data. Common cold-like symptoms (general malaise, slight fever, sore throat, etc.) preceded skin eruptions in 82% of the cases, and in all but 1 patient, the disease was accompanied by very high fever (more than 39° C) at the onset. It should be emphasized that acute conjunctivitis occurred before or simulta-

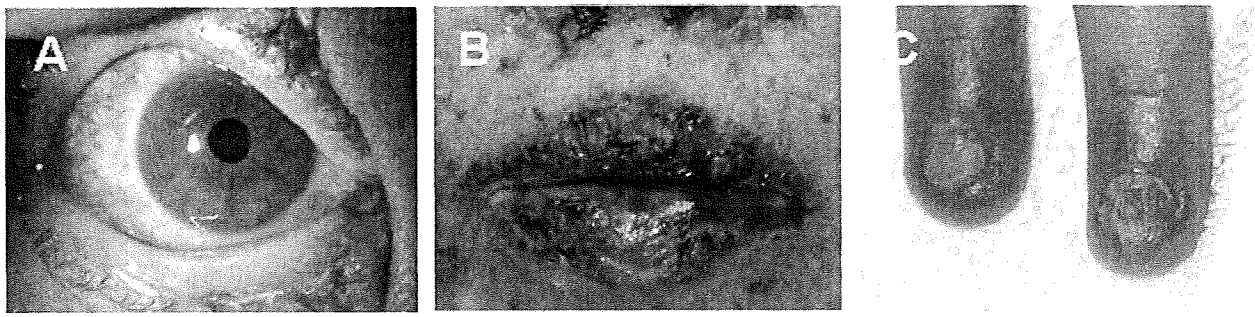

Figure 2. Representative photographs showing Stevens-Johnson syndrome/toxic epidermal necrolysis-associated ocular and oral involvement and fingernail loss at the acute stage. A, Conjunctivitis, which was accompanied by extensive loss of bulbar conjunctival epithelium. B, Swollen and crusted lips. C, Fingernail loss and deformation with paronychia.

neously with skin eruptions and that the involvement of oral mucosa was observed in 100% of the cases who could remember the details. Fingernail loss at the acute stage, deformation at the time of the writing of this report, or both also occurred in all of the patients, suggesting that paronychia occurred in all patients at the acute phase.

Visual outcomes were significantly better in the patients who received treatment with topical steroids during the first week from disease onset compared with those of the patients who received no topical steroid treatment. However, those outcomes may be because of the presumed fact that patients who fail to receive treatment with topical steroids are highly likely not going to receive systemic steroids as well. Thus, treatment with topical steroids, systemic steroids, or both at the early stage of the disease helps to decrease the incidence of chronic ocular complications. At the onset of the diseases, both necrotic changes of the skin and the destruction of the ocular surface progress rapidly. Prompt use of topical steroids, and presumably systemic steroids, from disease onset may prove to be important for preventing the loss of corneal epithelial stem cells. Unfortunately, a detailed history concerning the systemic therapy during the acute stage could not be obtained in most instances. Additional studies are needed to confirm the safety and efficacy of those medications.

Of the 94 patients, the mean duration of the illness was 16.1 years, and more than 50% of the eyes manifested visual acuity worse than 20/200. Considering the fact that patients with SJS or TEN experience ocular complications for an extended period, it is vital that strict attention be paid to any ocular involvement. When dermatologists, physicians, and healthcare professionals suspect SJS or TEN, prompt referral to an ophthalmologist is vital for the prevention of permanent loss of vision. Ophthalmologists have to find distinctive appearances such as pseudomembrane formation and corneal or conjunctival epithelial defects, or both.

Table 2. Order of Conjunctivitis and Skin Eruptions of the 94 Patients at Disease Onset

Conjunctivitis	Period Preceding Eruption	No. of Patients
Occurred before skin eruption	4 days	1
	3 days	3
	2 days	11
	1 day	12
	Several hours	9
	Unknown	6
		Total = 42
Occurred simultaneously		21
Occurred later		1
Unknown		30
Total		94

In the first report by Stevens and Johnson, 2 boys reported eye pain before skin eruptions and manifested a purulent conjunctivitis. Visual prognosis was total blindness in one case and severe corneal scarring in the other case. Both cases had the typical clinical picture clarified in the present study.[1] If their eyes had been treated with topical steroids from disease onset, the visual outcomes might have been different.

To date, the pathophysiologic mechanisms underlying the onset of SJS and TEN have yet to be fully elucidated. The rarity of these diseases has led us to speculate that patients with SJS or TEN genetically are susceptible to specific environmental precipitants. A report from the United States showed an increase of human leukocyte antigen (HLA)-B12 (HLA-Bw44) antigen in white patients with SJS with ocular involvement.[31] Analyses of TEN patients in France also disclosed an association with HLA-B12 (HLA-Bw44).[32] In Han Chinese, there was a very strong association between carbamazepine-induced SJS and the HLA-B*1502 allele.[33] The authors also reported that in Japanese persons, HLA-A*0206 was strongly associated with SJS and TEN with ocular surface complications.[34,38] These findings suggest that SJS and TEN are associated with a complex genetic inheritance background.

The prodromal symptoms occurred in 82% of the cases in this study. Given the association between the onset of SJS and TEN and infections and the opportunistic infection of ocular surfaces by bacteria such as methicillin-resistant *Staphylococcus aureus* or methicillin-resistant *Staphylococcus epidermidis*,[41] it is highly possible that there is an association between SJS and TEN and a disordered innate immune response. Recently, the association of the polymorphisms in the toll-like receptor 3 gene with SJS and TEN in the Japanese population were reported.[36] Also, an association between SJS and TEN and the IL-4R gene polymorphism and combined IL-13/IL-4R signaling pathway gene polymorphism was reported.[35,39]

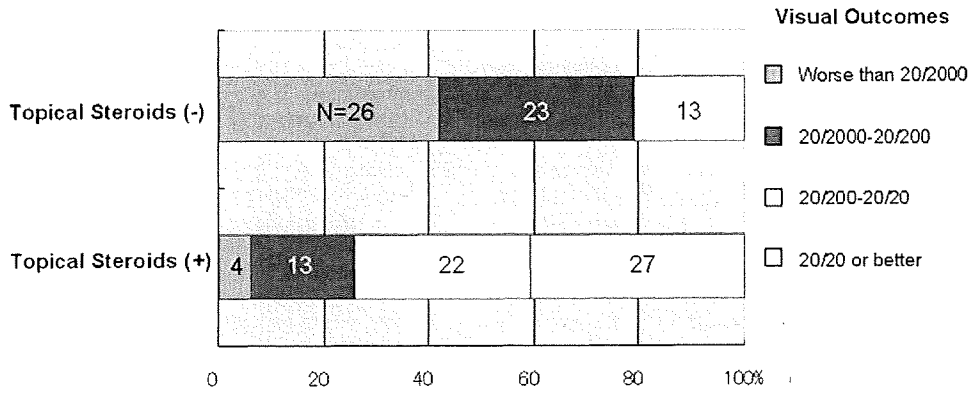

Figure 3. Graph showing the relationship between topical steroid use during the first week from disease onset and visual outcomes. Sixty-six eyes of 33 patients began topical steroid treatment during the first week from disease onset, whereas 62 eyes of 31 patients received no topical steroid treatment or any other treatment. Visual outcomes were significantly better in the group receiving topical steroids at the acute stage compared with those of the no-treatment group ($P<0.00001$).

Thus, both innate immunity and host-defense mechanisms may play a critical role in the development of SJS and TEN.

In conclusion, ocular involvement at disease onset is a helpful symptom for the diagnosis of SJS and TEN. Acute conjunctivitis before or occurring simultaneously with skin eruptions accompanied by very high fever and blisters on the mouth greatly implies the initial signs of SJS and TEN, and prodromal symptoms and genital involvements support that diagnosis. Initiating treatment with topical steroids from the onset seems to be important for the improvement of visual prognosis. A prompt and accurate diagnosis as assisted by the clinical manifestation offers a breakthrough against the historically poor visual outcomes associated with patients with SJS or TEN.

References

1. Stevens AM, Johnson FC. A new eruptive fever associated with stomatitis and ophthalmia: report of two cases in children. Am J Dis Child 1922;24:526–33.
2. Bastuji-Garin S, Rzany B, Stern RS, et al. Clinical classification of cases of toxic epidermal necrolysis, Stevens-Johnson syndrome, and erythema multiforme. Arch Dermatol 1993;129:92–6.
3. Roujeau JC. Stevens-Johnson syndrome and toxic epidermal necrolysis are severity variants of the same disease which differs from erythema multiforme. J Dermatol 1997;24:726–9.
4. Auquier-Dunant A, Mockenhaupt M, Naldi L, et al, SCAR Study Group. Correlations between clinical patterns and causes of erythema multiforme majus, Stevens-Johnson syndrome, and toxic epidermal necrolysis: results of an international prospective study. Arch Dermatol 2002;138:1019–24.
5. Roujeau JC, Stern RS. Severe adverse cutaneous reactions to drugs. N Engl J Med 1994;331:1272–85.
6. Roujeau JC, Kelly JP, Naldi L, et al. Medication use and the risk of Stevens-Johnson syndrome or toxic epidermal necrolysis. N Engl J Med 1995;333:1600–7.
7. Bachot N, Roujeau JC. Differential diagnosis of severe cutaneous drug eruptions. Am J Clin Dermatol 2003;4:561–72.
8. Yamane Y, Aihara M, Ikezawa Z. Analysis of Stevens-Johnson syndrome and toxic epidermal necrolysis in Japan from 2000 to 2006. Allergol Int 2007;56:419–25.
9. Mockenhaupt M, Viboud C, Dunant A, et al. Stevens-Johnson syndrome and toxic epidermal necrolysis: assessment of medication risks with emphasis on recently marketed drugs: the EuroSCAR-study. J Invest Dermatol 2008;128:35–44.
10. Power WJ, Ghoraishi M, Merayo-Lloves J, et al. Analysis of the acute ophthalmic manifestations of the erythema multiforme/Stevens-Johnson syndrome/toxic epidermal necrolysis disease spectrum. Ophthalmology 1995;102:1669–76.
11. Chang YS, Huang FC, Tseng SH, et al. Erythema multiforme, Stevens-Johnson syndrome, and toxic epidermal necrolysis: acute ocular manifestations, causes, and management. Cornea 2007;26:123–9.
12. Tugal-Tutkun I, Akova YA, Foster CS. Penetrating keratoplasty in cicatrizing conjunctival diseases. Ophthalmology 1995;102:576–85.
13. Sotozono C, Ang LP, Koizumi N, et al. New grading system for the evaluation of chronic ocular manifestations in patients with Stevens-Johnson syndrome. Ophthalmology 2007;114:1294–302.
14. Kawasaki S, Nishida K, Sotozono C, et al. Conjunctival inflammation in the chronic phase of Stevens-Johnson syndrome. Br J Ophthalmol 2000;84:1191–3.
15. Schermer A, Galvin S, Sun TT. Differentiation-related expression of a major 64K corneal keratin in vivo and in culture suggests limbal location of corneal epithelial stem cells. J Cell Biol 1986;103:49–62.
16. Cotsarelis G, Cheng SZ, Dong G, et al. Existence of slow-cycling limbal epithelial basal cells that can be preferentially stimulated to proliferate: implications on epithelial stem cells. Cell 1989;57:201–9.
17. Kinoshita S, Adachi W, Sotozono C, et al. Characteristics of the human ocular surface epithelium. Prog Retin Eye Res 2001;20:639–73.
18. Kinoshita S. The corneal epithelial stem cell puzzle: what future discoveries lie on the horizon? Arch Ophthalmol 2008;126:725–6.
19. Samson CM, Nduaguba C, Baltatzis S, Foster CS. Limbal stem cell transplantation in chronic inflammatory eye disease. Ophthalmology 2002;109:862–8.
20. Koizumi N, Inatomi T, Suzuki T, et al. Cultivated corneal epithelial stem cell transplantation in ocular surface disorders. Ophthalmology 2001;108:1569–74.
21. Koizumi N, Inatomi T, Suzuki T, et al. Cultivated corneal epithelial transplantation for ocular surface reconstruction in

acute phase of Stevens-Johnson syndrome. Arch Ophthalmol 2001;119:298–300.
22. Nakamura T, Ang LP, Rigby H, et al. The use of autologous serum in the development of corneal and oral epithelial equivalents in patients with Stevens-Johnson syndrome. Invest Ophthalmol Vis Sci 2006;47:909–16.
23. Ang LP, Sotozono C, Koizumi N, et al. A comparison between cultivated and conventional limbal stem cell transplantation for Stevens-Johnson syndrome. Am J Ophthalmol 2007;143: 178–80.
24. Nakamura T, Inatomi T, Sotozono C, et al. Transplantation of cultivated autologous oral mucosal epithelial cells in patients with severe ocular surface disorders. Br J Ophthalmol 2004; 88:1280–4.
25. Inatomi T, Nakamura T, Koizumi N, et al. Midterm results on ocular surface reconstruction using cultivated autologous oral mucosal epithelial transplantation. Am J Ophthalmol 2006; 141:267–75.
26. Inatomi T, Nakamura T, Kojyo M, et al. Ocular surface reconstruction with combination of cultivated autologous oral mucosal epithelial transplantation and penetrating keratoplasty. Am J Ophthalmol 2006;142:757–64.
27. Ang LP, Nakamura T, Inatomi T, et al. Autologous serum-derived cultivated oral epithelial transplants for severe ocular surface disease. Arch Ophthalmol 2006;124:1543–51.
28. Lehman SS. Long-term ocular complication of Stevens-Johnson syndrome. Clin Pediatr (Phila) 1999;38:425–7.
29. Hynes AY, Kafkala C, Daoud YJ, Foster CS. Controversy in the use of high-dose systemic steroids in the acute care of patients with Stevens-Johnson syndrome. Int Ophthalmol Clin 2005;45:25–48.
30. Schneck J, Fagot JP, Sekula P, et al. Effects of treatments on the mortality of Stevens-Johnson syndrome and toxic epidermal necrolysis: a retrospective study on patients included in the prospective EuroSCAR Study. J Am Acad Dermatol 2008; 58:33–40.
31. Mondino BJ, Brown SI, Biglan AW. HLA antigens in Stevens-Johnson syndrome with ocular involvement. Arch Ophthalmol 1982;100:1453–4.
32. Roujeau JC, Huynh TN, Bracq C, et al. Genetic susceptibility to toxic epidermal necrolysis. Arch Dermatol 1987;123: 1171–3.
33. Chung WH, Hung SI, Hong HS, et al. Medical genetics: a marker for Stevens-Johnson syndrome. Nature 2004;428:486.
34. Ueta M, Sotozono C, Tokunaga K, et al. Strong association between *HLA-A*0206* and Stevens-Johnson syndrome in the Japanese. Am J Ophthalmol 2007;143:367–8.
35. Ueta M, Sotozono C, Inatomi T, et al. Association of *IL4R* polymorphisms with Stevens-Johnson syndrome [letter]. J Allergy Clin Immunol 2007;120:1457–9.
36. Ueta M, Sotozono C, Inatomi T, et al. Toll-like receptor 3 gene polymorphisms in Japanese patients with Stevens-Johnson syndrome. Br J Ophthalmol 2007;91:962–5.
37. Lonjou C, Borot N, Sekula P, et al, RegiSCAR Study Group. A European study of HLA-B in Stevens-Johnson syndrome and toxic epidermal necrolysis related to five high-risk drugs. Pharmacogenet Genomics 2008;18:99–107.
38. Ueta M, Tokunaga K, Sotozono C, et al. HLA class I and II gene polymorphisms in Stevens-Johnson syndrome with ocular complications in Japanese. Mol Vis 2008;14:550–5.
39. Ueta M, Sotozono C, Inatomi T, et al. Association of combined IL-13/IL-4R signaling pathway gene polymorphism with Stevens-Johnson Syndrome accompanied by ocular surface complications. Invest Ophthalmol Vis Sci 2008;49:1809–13.
40. Kaniwa N, Saito Y, Aihara M, et al, JSAR Research Group. HLA-B locus in Japanese patients with anti-epileptics and allopurinol-related Stevens-Johnson syndrome and toxic epidermal necrolysis. Pharmacogenomics 2008;9:1617–22.
41. Sotozono C, Inagaki K, Fujita A, et al. Methicillin-resistant *Staphylococcus aureus* and methicillin-resistant *Staphylococcus epidermidis* infections in the cornea. Cornea 2002;21(suppl):S94–101.

Footnotes and Financial Disclosures

Originally received: September 4, 2008.
Final revision: November 26, 2008.
Accepted: December 18, 2008.
Available online: February 25, 2009. Manuscript no. 2008-1063.

[1] Department of Ophthalmology, Kyoto Prefectural University of Medicine, Kyoto, Japan.

[2] Department of Dermatology, Ehime University School of Medicine, Ehime, Japan.

[3] Department of Environmental Immuno-Dermatology, Yokohama City University Graduate School of Medicine, Kanagawa, Japan.

Financial Disclosure(s):
The author(s) have no proprietary or commercial interest in any materials discussed in this article.

Supported in part by Health and Labor Sciences Research Grants (Research on Intractable Diseases) from the Ministry of Health, Labour and Welfare of Japan, Tokyo, Japan; the Japanese Ministry of Education, Culture, Sports, Science and Technology, Tokyo, Japan; the Kyoto Foundation for the Promotion of Medical Science, Kyoto, Japan; and the Intramural Research Fund of Kyoto Prefectural University of Medicine, Kyoto, Japan.

Correspondence:
Chie Sotozono, MD, PhD, Department of Ophthalmology, Kyoto Prefectural University of Medicine, Kawaramachi Hirokoji, Kamigyo-ku, Kyoto 602-0841, Japan. E-mail: csotozon@koto.kpu-m.ac.jp.

Disclosure of potential conflict of interest: A. P. Kaplan is a consultant for Lev Pharmaceuticals and Sanofi-Aventis and receives research support from Lev Pharmaceuticals and Novartis Pharmaceuticals.

REFERENCES

1. Kessel A, Toubi E. Low-dose cyclosporine is a good option for severe chronic urticaria. J Allergy Clin Immunol 2009;123:970.
2. Kaplan AP. What the first 10,000 patients with chronic urticaria have taught me: a personal journey. J Allergy Clin Immunol 2009;123:713-7.
3. Kaplan AP, Joseph K, Maykut RJ, Geba GP, Zeldin RK. Treatment of chronic autoimmune urticaria with omalizumab. J Allergy Clin Immunol 2008;122:569-73.

doi:10.1016/j.jaci.2009.01.067

The influence of hepatic damage on serum soluble Fas ligand levels of patients with drug rashes

To the Editor:

We read with interest the report of Murata et al[1] stating that increases in soluble Fas ligand (sFasL) levels were observed in patients with Stevens-Johnson syndrome (SJS) and toxic epidermal necrolysis (TEN) in the very early phases but not in maculopapular (MP) types of drug rash. However, we reported recently that increases in serum sFasL levels were observed not only in patients with SJS and TEN but also in those with drug-induced hypersensitivity syndrome (DIHS) and MP-type drug eruptions.[2] Examinations were performed in groups of 4 patients each, and the changes in sFasL levels showed a similar pattern among all 3 types of drug rash. The sFasL levels peaked within a week after onset of the rash and then decreased rapidly thereafter. These observations suggested that increases in sFasL levels in patients with drug rashes are not a specific indicator of SJS/TEN. To further confirm this suggestion, we focused on serum sFasL levels within 5 days after onset of drug rash and examined a larger number of cases.

Serum samples were collected from patients with DIHS, MP-type drug rash, erythema multiforme (EM)–type drug rash, SJS, and TEN and subjected to clinical laboratory testing within 5 days of onset. Nineteen serum samples from 13 patients with DIHS, 37 serum samples from 31 patients with MP/EM-type drug rashes, and 13 serum samples from 11 patients with SJS/TEN, which excluded 12 cases reported previously from this examination, were examined. The highest sFasL level was chosen in each patient. sFasL levels were measured with an ELISA kit (R&D Systems, Minneapolis, Minn), and the detection limit was 16 pg/mL. The average sFasL level of patients with SJS/TEN was 96 ± 29 pg/mL, which was similar to that of 16 healthy control subjects (90 ± 59 pg/mL). However, the sFasL levels of patients with DIHS and MP/EM-type drug rashes were significantly higher (patients with DIHS: 214 ± 127 pg/mL, $P = 0.0082$; patients with MP/EM-type drug rashes: 160 ± 81 pg/mL, $P = .0012$) than those of healthy control subjects and patients with SJS/TEN. This result was in agreement with the findings of our previous study.[2]

The Fas–Fas ligand (FasL) system mediates hepatocyte apoptosis in various liver diseases.[3] Upregulated Fas on hepatocytes is engaged with FasL expressed on cytotoxic T cells, inducing apoptosis of hepatocytes.[4] As FasL is shed and released into the serum,[5] serum sFasL levels are increased in patients with acute and fulminant hepatitis.[6,7] Because all patients with DIHS and many patients with MP/EM-type drug rashes were associated with liver dysfunction in the present study, we speculated that the increases in sFasL levels in these patients reflected liver damage. Increases in alanine aminotransferase (ALT) levels within 5 days of onset were observed in 31 of 55 patients. Interestingly, 14 cases in which serum ALT levels were increased by more than 5-fold compared with the normal limit showed significantly increased sFasL levels (Fig 1). In addition, all patients with sFasL levels of greater than 300 pg/mL were associated with increased ALT levels of greater than 5-fold compared with the normal limit.

Taken together, these observations indicate that increase of serum sFasL levels is not specific for SJS and TEN. Rather, higher sFasL levels might indicate hepatic damage. Therefore these values should not be used as an indicator of the development of SJS or TEN.

Mikiko Tohyama, MD
Yuji Shirakata, MD, PhD
Koji Sayama, MD, PhD
Koji Hashimoto, MD, PhD

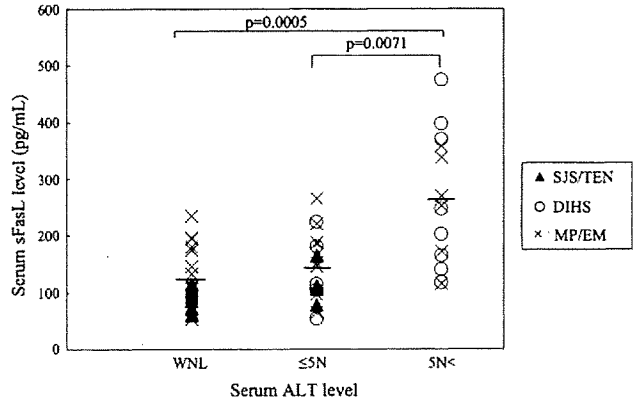

FIG 1. In 24 of 55 patients, serum ALT levels were within normal limits *(WNL)* until 5 days after onset. Increases in ALT levels of 5-fold or less compared with the normal limit *(≤5N)* and of greater than 5-fold compared with the normal limit *(5N<)* were observed in 17 and 14 patients, respectively. The Student *t* test was used for comparison of paired conditions.

From the Department of Dermatology, Ehime University Graduate School of Medicine, Toon-city, Ehime, Japan. E-mail: tohm@m.ehime-u.ac.jp.
K.H. received grant support from Health Sciences Research Grants for Research on Specific Diseases from the Ministry of Health, Labor, and Welfare of Japan.
Disclosure of potential conflict of interest: The authors have declared that they have no conflict of interest.

REFERENCES
1. Murata J, Abe R, Shimizu H. Increased soluble Fas ligand levels in patients with Stevens-Johnson syndrome and toxic epidermal necrolysis preceding skin detachment. J Allergy Clin Immunol 2008;122:992-1000.
2. Tohyama M, Shirakata Y, Sayama K, Hashimoto K. A marked increase in serum soluble Fas ligand in drug-induced hypersensitivity syndrome. Br J Dermatol 2008; 159:981-4.
3. Guicciardi ME, Gores GJ. Apoptosis: a mechanism of acute and chronic liver injury. Gut 2005;54:1024-33.
4. Nagata S, Golstein P. The Fas death factor. Science 1995;267:1449-56.
5. Tanaka M, Itai T, Adachi M, Nagata S. Downregulation of Fas ligand by shedding. Nat Med 1998;4:31-6.
6. Ryo K, Kamogawa Y, Ikeda I, Yamauchi K, Yonehara S, Nagata S, et al. Significance of Fas antigen-mediated apoptosis in human fulminant hepatic failure. Am J Gastroenterol 2000;95:2047-55.
7. Tokushige K, Yamaguchi N, Ikeda I, Hashimoto E, Yamauchi K, Hayashi N. Significance of soluble TNF receptor-I in acute-type fulminant hepatitis. Am J Gastroenterol 2000;95:2040-6.

doi:10.1016/j.jaci.2009.01.064

Reply

To the Editor:

We thank Dr Tohyama et al[1] for their interest in our study.[2] They reported that the difference of serum soluble Fas ligand (sFasL) levels between patients with toxic epidermal necrolysis (TEN)/Stevens-Johnson syndrome (SJS) and maculopapular types of drug rash was not observed.[1,3] This observation is in contrast to our study, in which we detected the highest concentrations of sFasL in 71.4% of patients with TEN/SJS before disease onset (approximately day −4 to −2). Increased sFasL levels decreased rapidly within 5 days of disease onset. In all of 32 patients with ordinary types of drug-induced skin reactions (ODSR), no increase in sFasL level was detected.[2,4]

Several molecules have been reported as important mediators in the pathogenesis of TEN/SJS. A very recent article reported that granulysin is a key molecule responsible for the development of TEN/SJS. In this article it was also shown that sFasL is confirmed as a highly expressed molecule in patients with TEN/SJS.[5]

Several points are warranted in the interpretation of the results of Tohyama et al.[1] In particular, we reported that sFasL levels were decreased after day 3.[2] Detailed information on sample collection was not described in the correspondence by Tohyama et al.[1] If the serum samples were collected after day 3, sFasL levels should have returned to within the normal range. We have to emphasize that it is very difficult to distinguish clinical presentations of TEN/SJS at the early stage from ODSR. Therefore it is crucial to collect and analyze the samples of TEN/SJS at an early stage.

Additionally, in the correspondence by Tohyama et al,[1] serum levels of sFasL seemed to be higher than those seen in our study. In our study sFasL levels of healthy control subjects were 42.8 ± 8.2 pg/mL,[2] whereas they were 90 ± 59 pg/mL in Tohyama et al.[1]

Furthermore, Tohyama et al[1] used a different definition of disease onset of TEN/SJS compared with ours. A major previous report defined disease onset as when erosion/ulceration of mucocutaneous or ocular lesions are first developed,[6] and we followed that precedent. In contrast, in Tohyama et al's correspondence,[1] onset is defined as the day when the rash appears. It is well known that the disease course of TEN/SJS is variable; some patients have erosion/ulceration without erythema, and other show only erythema for several days before erosion/ulceration appears. Because erosion/ulceration or ocular lesions are essential manifestations of TEN/SJS, the presence of markers such as sFasL or granulysin to distinguish the early stage of TEN/SJS from ODSR is crucial.

Riichiro Abe, MD, PhD
Junko Murata, MD
Naoya Yoshioka, MS
Hiroshi Shimizu, MD, PhD

From the Department of Dermatology, Hokkaido University Graduate School of Medicine, Sapporo, Japan. E-mail: shimizu@med.hokudai.ac.jp or aberi@med.hokudai.ac.jp.
Disclosure of potential conflict of interest: The authors have declared that they have no conflict of interest.

REFERENCES
1. Tohyama M, Shirakata Y, Sayama K, Hashimoto K. The influence of hepatic damage on serum soluble Fas ligand levels of patients with drug rashes. J Allergy Clin Immunol 2009;123:971-2.
2. Murata J, Abe R, Shimizu H. Increased soluble Fas ligand levels in patients with Stevens-Johnson syndrome and toxic epidermal necrolysis preceding skin detachment. J Allergy Clin Immunol 2008;122:992-1000.
3. Tohyama M, Shirakata Y, Sayama K, Hashimoto K. A marked increase in serum soluble Fas ligand in drug-induced hypersensitivity syndrome. Br J Dermatol 2008;159:981-4.
4. Abe R, Shimizu T, Shibaki A, Nakamura H, Watanabe H, Shimizu H. Toxic epidermal necrolysis and Stevens-Johnson syndrome are induced by soluble Fas ligand. Am J Pathol 2003;162:1515-20.
5. Chung WH, Hung SI, Yang JY, Su SC, Huang SP, Wei CY, et al. Granulysin is a key mediator for disseminated keratinocyte death in Stevens-Johnson syndrome and toxic epidermal necrolysis. Nat Med 2008;14:1343-50.
6. Roujeau JC, Kelly JP, Naldi L, Rzany B, Stern RS, Anderson T, et al. Medication use and the risk of Stevens-Johnson syndrome or toxic epidermal necrolysis. N Engl J Med 1995;333:1600-7.

doi:10.1016/j.jaci.2009.01.066

Activation of the blood coagulation cascade is involved in patients with chronic urticaria

To the Editor:

Chronic urticaria (CU) is a continuously recurrent whealing of the skin with pruritus and usually defines its course as 6 weeks and more. As reported in the JACI, Asero et al[1] found that the tissue factor pathway of blood coagulation might be active in patients with CU.

Thirty adult patients (men/women, 11/19; median age, 40.88 years; range, 18-66 years) with CU and 30 normal subjects (men/women, 11/19; median age, 39.93 years; range, 18-58 years) were enrolled in the study. Disease activity was estimated according to the number of wheals presented. Prothrombin time (PT) and partial thromboplastin time (APTT) were measured by the coagulation method (Dade Behring Marburg GmbH, Marburg, Germany). The level of D-dimer was tested with a turbidimetric immunoassay kit (Dade Behring Marburg GmbH). Levels of plasma activated Factor VII (FVIIa) and thrombin-antithrombin complex (TAT) were measured by ELISA kit (FVIIa: American Diagnostic Inc, Stanford, Conn; TAT: AssayPro, St Charles, Mo). Means were compared by *t* test. Differences in the levels of FVIIa, TAT, and D-dimer were assessed by the Wilcoxon-Mann-Whitney nonparametric test. Correlations between the various parameters were assessed by the Spearman test.

Disease activity of patients was graded as slight, 4; moderate, 11; severe, 7; and very severe, 8. The results in Table I show that PT and APTT were in the normal range, and the levels of FVIIa,

Molecular Vision 2009; 15:937-948 <http://www.molvis.org/molvis/v15/a98>
Received 24 February 2009 | Accepted 23 April 2009 | Published 8 May 2009

Alteration of TLR3 pathways by glucocorticoids may be responsible for immunosusceptibility of human corneal epithelial cells to viral infections

Yuko Hara,[1] Atsushi Shiraishi,[2] Takeshi Kobayashi,[2] Yuko Kadota,[1] Yuji Shirakata,[3] Koji Hashimoto,[3] Yuichi Ohashi[1]

[1]Department of Ophthalmology, Ehime University School of Medicine, Shitsukawa, Japan; [2]Department of Ophthalmology and Regenerative Medicine, Ehime University School of Medicine, Shitsukawa, Japan; [3]Department of Dermatology, Ehime University School of Medicine, Shitsukawa, Japan

Purpose: The toll-like receptor 3 (TLR3) recognizes viral double-stranded RNA and its synthetic analog polyriboinosinic-polyribocytidylic acid (poly(I:C)), and the activation of TLR3 is known to induce the production of type I interferon (IFN) and inflammatory cytokines/chemokines. The purpose of this study was to determine the role played by innate responses to a herpes simplex virus 1 (HSV-1) infection of the corneal epithelial cells. In addition, we determined the effects of immunosuppressive drugs on the innate responses.Methods: Cultured human corneal epithelial cells (HCECs) were exposed to poly(I:C), and the expressions of the mRNAs of the cytokines/chemokines macrophage-inflammatory protein 1 alpha (*MIP1-α*), macrophage-inflammatory protein 1 beta (*MIP1-β*), interleukin-6 (*IL-6*), interleukin-8 (*IL-8*), regulated on activation, normal T cell expressed and secreted (*RANTES*), Interferon-beta (*IFN-β*), and *TLR3* were determined using real-time reverse transcription-polymerase chain reaction (RT-PCR). The effects of dexamethasone (DEX, 10^{-6} or 10^{-5} M) and cyclosporine A (CsA, 10^{-6} or 10^{-5} M) on the expression of these cytokines and *TLR3* were also determined using real-time RT-PCR. Levels of MIP1-α, MIP1-β, IL-6, IL-8, RANTES, and IFN-β were measured using the enzyme-linked immunosorbent assay (ELISA). The activation of nuclear factor kappa B (NFκB) and interferon regulatory factor 3 (IRF3) in HCECs was assessed by immunohistochemical staining. The effects of DEX and CsA on HCECs exposed to HSV-1 (McKrae strain) were also examined.Results: The expressions of *MIP1-α*, *MIP1-β*, *IL-6*, *IL-8*, *RANTES*, *IFN-β*, and *TLR3* were up-regulated in HCECs exposed to poly(I:C). The poly(I:C)-induced expressions of *IL-6* and *IL-8* were down-regulated by both DEX and CsA, while the expressions of *IFN-β* and *TLR3* were suppressed by DEX alone. Similarly, the poly(I:C)-induced activation of NFκB was decreased by both DEX and CsA, and the activation of IRF3 was reduced by DEX alone. When HCECs were inoculated with HSV-1, DEX led to a decrease in the expression of *IL6*, *IFN-β*, and *TLR3*, and an extension of plaque formation.Conclusion: These results indicate that DEX may increase the susceptibility of HCECs to viral infections by altering the TLR3 signaling pathways.

The toll-like receptors (TLRs) are a family of innate immune receptors that recognize the conserved structures of microbes, termed pathogen-associated molecular patterns (PAMPs). The TLR system has been extensively studied in immune cells, e.g. in macrophages, and recent studies have demonstrated that epithelial cells also express TLRs. Thus, respiratory epithelial cells express TLR 1–10 [1,2], epidermal keratinocytes express TLR1, 2, 4, and 5 [3,4], intestinal epithelial cells express TLR1–4, 6, and 9 [5], and female reproductive tract epithelial cells express TLR1–9 [6]. In the eye, human corneal epithelial cells express TLR 1–7, 9, and 10 [7], and human conjunctival epithelial cells express TLR 1–6 and 9 [8].

The question then arises whether the TLRs play a role in the keratitis caused by the herpes simplex virus (HSV). It is known that treatment of stromal keratitis with topical acyclovir significantly reduces the number of patients who suffer serious visual impairment. However, keratitis often recurs in immunocompromised hosts or in individuals who receive steroid therapy for a long period of time. In fact, topical or systemic application of glucocorticoids results in the reactivation of herpes keratitis [9,10], and glucocorticoids are contraindicated for epithelial keratitis because they can worsen the clinical course to virus-induced geographic keratitis [11].

Recent studies have shown that a TLR3 ligand, which is a double-stranded RNA (dsRNA) can activate different types of epithelial cells, e.g. airway epithelial cells, female reproductive tract epithelial cells, and corneal epithelia cells [7,12,13]. TLR3 is the only TLR that does not interact with myeloid differentiation factor 88 (MyD88) as a signaling adaptor [14]. TLR3 interacts directly with the adaptor protein, Toll/interleukin-1 receptor (TIR) domain-containing adaptor inducing IFN-β (TRIF), which is also called the TIR-

Correspondence to: Yuko Hara, Department of Ophthalmology, Ehime University School of Medicine Shitsukawa, Toon, Ehime 791-0295, Japan; Phone: 81-89-960-5361; FAX: 81-89-960-5364; email: yukoabc@m.ehime-u.ac.jp